ФИЗИКА ЭЛЕМЕНТАРНЫХ ЧАСТИЦ И АТОМНОГО ЯДРА
2011. Т. 42. ВЫП. 4

ACCELERATOR NEUTRINO PHYSICS — CURRENT STATUS AND FUTURE PROSPECTS

S. G. Wojcicki

Stanford University, Stanford, CA, USA

ФИЗИКА ЭЛЕМЕНТАРНЫХ ЧАСТИЦ И АТОМНОГО ЯДРА
2011. Т. 42. ВЫП. 4

ACCELERATOR NEUTRINO PHYSICS — CURRENT STATUS AND FUTURE PROSPECTS

S. G. Wojcicki

Stanford University, Stanford, CA, USA

This review article describes the current status and future prospects of accelerator neutrino physics. The emphasis is on recent developments in the oscillation physics area, but there is also a limited discussion about the status of neutrino cross sections. The approach taken is pedagogical, and an effort is made to explain the basic techniques used in the accelerator studies of neutrino physics.

PACS: 14.60.Pq; 95.55.Vj

INTRODUCTION

The neutrinos are ubiquitous in nature. They are not only produced constantly in natural phenomena like the burning of the Sun, explosion of supernovas, decays of cosmic ray secondaries, and decays of radioactive elements in the air, on the Earth's surface and deep inside the Earth but also are believed to have been created some 13 billion years ago in the Big Bang. Furthermore, they can be produced in or by man-made sources: reactors, nuclear explosions, accelerators, and artificially produced radioactive isotopes.

Given the multiplicity of neutrino sources, it is not surprising that they cover a very broad energy spectrum, different sources being generally characterized by neutrinos of a characteristic spectrum and of different intensity. At one extreme are the cosmological neutrinos created in the Big Bang with present flux of about $10^{22}/(\mathrm{cm}^2 \cdot \mathrm{s} \cdot \mathrm{sr} \cdot \mathrm{MeV})$ and energies in the μeV to meV range. On the other extreme are the so-called GZK neutrinos with fluxes in the $10^{-26}/(\mathrm{cm}^2 \cdot \mathrm{s} \cdot \mathrm{sr} \cdot \mathrm{MeV})$ and energies in the PeV to EeV range. Our current knowledge of neutrino physics is based on a wide range of studies of neutrinos from different sources. This diversity of spectra and sources has allowed us to probe the nature of neutrinos in surprisingly great detail.

Accelerator experiments have played a very important role in developing our current understanding of neutrinos. This was due to the versatility and flexibility of neutrino accelerator experiments, the ability to control the flavor and energy of the neutrinos and, very importantly, many technological improvements in this general area. This paper will attempt to briefly map out this history and these features, describe the recent advances, and summarize the future prospects.

1. BASICS OF ACCELERATOR NEUTRINO EXPERIMENTS

The first ideas to use decays of pions produced in accelerators as the source of neutrinos was independently due to B. Pontecorvo [1] and M. Schwartz [2]. Pontecorvo focused on studying potential anomalies in ν_μ interactions while Schwartz saw this primarily as a way of studying weak interactions without any significant interference from the much stronger weak and strong forces. The first accelerator experiment which succeeded in observing neutrinos was the one at Brookhaven by the Columbia group which also was able to show that ν_μ and ν_e had different interactions and hence were distinct [3].

The Brookhaven experiment was quite primitive by the today's standards. The primary proton beam struck an internal target and no focusing was used. Accordingly the fluxes were relatively modest and there was no significant separation between neutrinos and antineutrinos. In the subsequent years, the two most important technical developments relevant for neutrino studies were invention and development of neutrino horns and mastery of clean extraction of the circulating proton beam. Neutrino horn, so called because of its typical horn-like shape, was basically a configuration of two conductors where a flow of electric current would generate toroidal magnetic field. Thus, depending on the direction of the current, either positive or negative particles would be focused (the others being defocused), and hence the resulting flux was predominantly either neutrinos or antineutrinos. The horns were pulsed in synchronism with the extracted beam with typical currents of around 200 kA. The ability to extract the proton beams enabled much better shielding and thus lowered irradiation of neighboring elements (and hence made higher intensities possible), allowed more flexibility in targeting and focusing, and gave possibility of producing parent meson beams at 0° with respect to the proton beam which further increased the overall neutrino intensities.

The standard and most frequently used neutrino beams, are produced from decays of pions and kaons, with the dominant two-body decays into π and ν_μ providing most of the flux. Neutrinos originating from K decays give a higher energy flux, their energies reaching close to the energy of the parent kaon; on the other hand, the neutrinos from pion decays are limited kinematically to at most 42% of the parent pion energy. An important additional component in standard beams are ν_es originating either from the three-body decays of the kaons (branching ratio about 5%) or from tertiary muon decays.

Even in the standard, horn focused beam, commonly referred to as a wide band beam, one can control to a certain extent the energy spectrum of the produced neutrinos. This is done by adjusting the longitudinal position of the target with respect to the first magnetic horn. Furthermore, the combination of that position and the value of the generated magnetic field determine the range of the production transverse momenta of the parents that are most effectively focused. As an

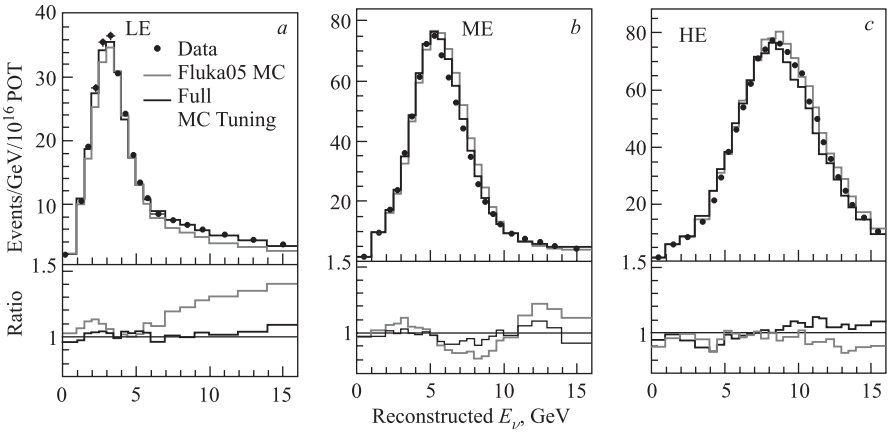

Fig. 1. NuMI CC event rates for different target locations: 10, 100, and 250 cm (corresponding roughly to the distance between the downstream end of the target and the point 20 cm upstream of the neck of the first horn) together with the MC predictions, before and after tuning. The data/MC ratios for these two MC predictions are indicated at the bottom

example, in Fig. 1 we show the energy spectrum of the NuMI beam at Fermilab for three different distances between the target and the first horn.

In the intervening time since the first neutrino experiment there were a number of other variations of the basic concept of neutrino beam that have been used in such experiments. Very briefly they were:

• Bare target beams, like the original BNL experiment. They allow somewhat cleaner determination of the neutrino flux since no focusing is involved but one pays penalty in the total intensity.

• Sign selected beam, where one uses a dipole to cleanly reject the parents of unwanted sign.

• Narrow band beam, where one selects the accepted momentum bite of the parent mesons.

• Beam dump «beam», where one tries to minimize as much as possible the available decay region for the parent mesons.

• Off-axis beam where the accepted neutrinos come off at a nonzero angle with respect to the initial proton (and accepted mesons) direction. Such an arrangement gives a rather narrow energy spectrum with an intensity at the chosen energy that is significantly higher than would be obtained in a wide band beam.

Determination of neutrino energy spectrum presents unique challenges that are not present in a typical charged particle beam or even neutral hadron beam.

In principle, the flux of neutrinos can be determined with the help of auxiliary experiment(s) which measures the production of hadrons by protons of the comparable energy to that used in the neutrino experiment. The resulting neutrino flux can then be derived using Monte Carlo simulations from those measurements, knowledge of the beam geometry and the properties of the focusing system.

In practice, however, that is quite difficult. The hadronic production experiments performed to date have suffered from inadequate statistics, lack of coverage of the complete required final-state phase space and/or somewhat different proton energies and target geometries, requiring additional complex extrapolations and simulations. The method that is generally adopted in long baseline neutrino experiments is to use two detectors, the first one relatively close to the target and the second one at a distance appropriate for the desired oscillation measurement. In this configuration, the near detector is used to measure the flux times cross section by observing the rate of (generally charged current — CC) interactions as a function of energy and then extrapolating those measurements to the far detector. Some Monte Carlo calculations are still needed to make this extrapolation but the level of the required knowledge of proper Monte Carlo input is relatively modest in this approach. Many of the uncertainties like those regarding detailed flux knowledge and energy dependence of cross sections cancel in this procedure.

There is some ambiguity as to the optimal features of the near detector. On the one hand, one wants the detector to be as similar in its internal construction as the far detector so as to eliminate or reduce most of the uncertainties inherent in the extrapolation. On the other hand, one also wants it to have the capability to measure the nature of the interactions in as detailed a way as possible. The ideal solution would be to have two near detectors, each one optimized for different

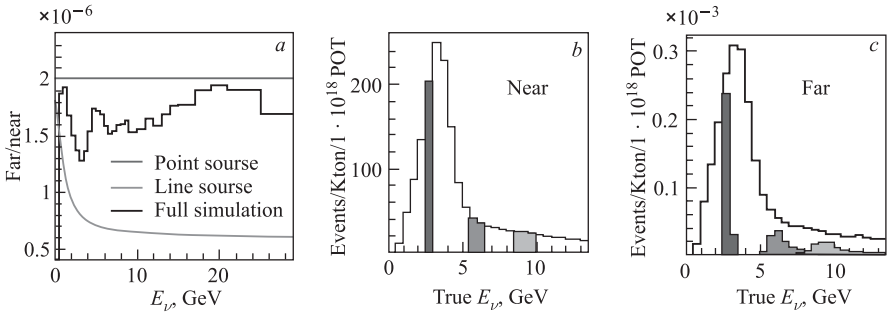

Fig. 2. Far/near ratio for the NuMI beam. *a*) These ratios for the actual case and for a line source and a point source. Plots *b* and *c* show how the different bands of neutrino energies in the near detector extrapolate to the far detector

function, but that is seldom adopted due to the pressures to keep low the total cost of the experiment. Different experiments constructed so far have adopted different solutions.

Figure 2 shows the details of the Near/Far extrapolation for the NuMI beam in the MINOS experiment. The relationship between the two is given by

$$N_{\mathrm{FD}}^{\mathrm{pred}} = (N_{\mathrm{FD}}^{\mathrm{MC}}/N_{\mathrm{ND}}^{\mathrm{MC}})N_{\mathrm{ND}}^{\mathrm{obs}}. \quad (1)$$

The ratio has an energy dependence which is illustrated in Fig. 2, *a* and is due to the fact that we have a line source for neutrinos and hence different acceptance ratio for the near detector depending on the point of decay. Plot *c* shows the far detector neutrino spectrum generated by the parent mesons giving neutrinos in a small energy band in the near detector as shown in Fig. 2, *b*.

2. STUDIES OF DOMINANT OSCILLATION PARAMETERS IN THE ATMOSPHERIC SECTOR

The neutrino oscillations in the atmospheric domain are dominated by two parameters, the mass squared difference, Δm^2_{13}, and mixing angle $\sin^2(2\theta_{23})$. Typical experiment looks for disappearance of ν_μs via detection of their CC interactions. The formula, in the two-flavor approximation, for the ν_μ survival probability, is given by

$$P(\nu_\mu \to \nu_\mu) = 1 - \sin^2(2\theta)\sin^2(1.27\Delta m^2 L/E). \quad (2)$$

The parameters are generally extracted by a simultaneous fit to both of them but different features of the energy spectrum tend to determine each one. The mass squared difference is determined principally by the location of the dip in the ratio of the observed to predicted number of events; the mixing angle is governed by the depth of this dip. This is illustrated in Fig. 3, where we have used arbitrary values of these two parameters, namely $\Delta m^2_{13} = 3.35 \cdot 10^{-3}$ eV^2 and mixing angle $\sin^2(2\theta_{23}) = 1$. The first long baseline neutrino experiment was the K2K in Japan where neutrinos were produced by a beam from the KEK 12 GeV proton synchrotron and detected by Super-Kamiokande water Cherenkov detector 225 km away [4]. There were two near detectors used. One of them was a smaller water Cherenkov counter, the other — a fine grained detector. The experiment suffered from low statistics but nevertheless was able to demonstrate energy-dependent disappearance of muon neutrinos which was consistent with the oscillation hypothesis with oscillation parameters in agreement with those measured by the Super-Kamiokande in its investigation of atmospheric neutrinos. The oscillation parameters were extracted independently both from the overall

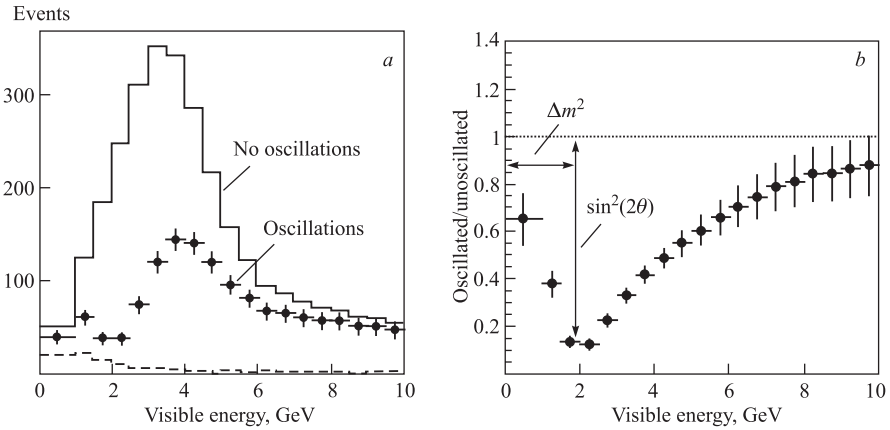

Fig. 3. An example of the effect of oscillations using MC calculations. The rates without and with oscillations are shown on the plot *a* and their ratio on the plot *b*. That figure also indicates the features of this ratio curve that mainly determine the oscillation parameters

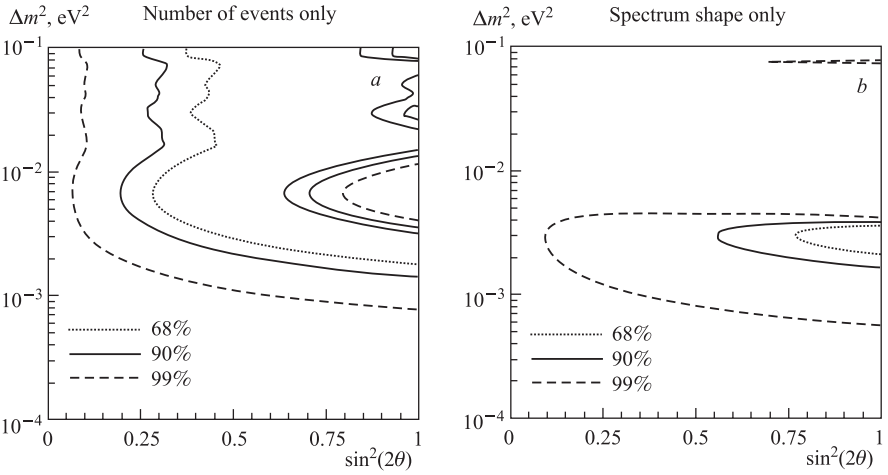

Fig. 4. The allowed oscillation parameter space for the K2K experiment obtained from the event rate only (*a*) and from the spectrum shape only (*b*)

CC event rate in the Super-Kamiokande and from shape-only spectrum, the latter providing better constraints as indicated in Fig. 4. The best measurement was obtained from the energy spectrum of 58 single ring ν_μ events as shown in Fig. 5.

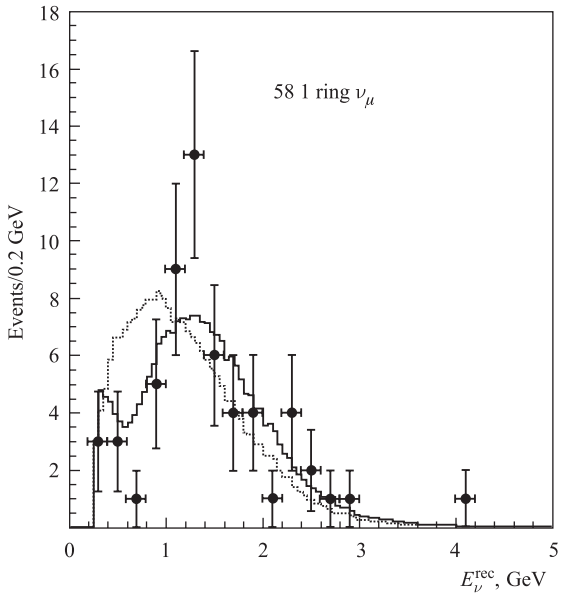

Fig. 5. The measured K2K spectrum using the 1 ring ν_μ events only. Superimposed are the best fits with oscillations (solid) and without oscillations (dotted)

MINOS experiment was designed for more detailed investigation of the atmospheric sector [5]. It uses the NuMI beam at Fermilab, produced by the 120 GeV protons from the Main Injector accelerator. The principal (far) detector of 5.4 kt is located in a former iron mine in Soudan, MN, at a distance of 725 km from the target. A smaller (near), 980 t detector is located 1.04 km from the target, at Fermilab, and serves to provide a detailed measurement of the neutrino flux at that site. The principal oscillation measurement is done with the beam tuned to low energy, peaking at about 3 GeV. Shorter runs at several different energies were made to obtain better constraints on the p_T and p_z distributions of the parent hadrons and thus better accuracy in extrapolating the neutrino spectrum to the far detector.

The experiment has been designed to optimize the measurement of the ν_μ disappearance via its charged current interactions [6]. Thus the design choice was to optimize the total tonnage at the expense of fine granularity. The detectors are iron scintillator calorimeters with a toroidal magnetic field averaging about 1.2 T. The general structure is alternating planes of iron, 2.5 cm thick, and scintillator planes composed of 4.1 cm wide strips whose orientation changes by 90° in successive planes. The two detectors have the same transverse and longitudinal

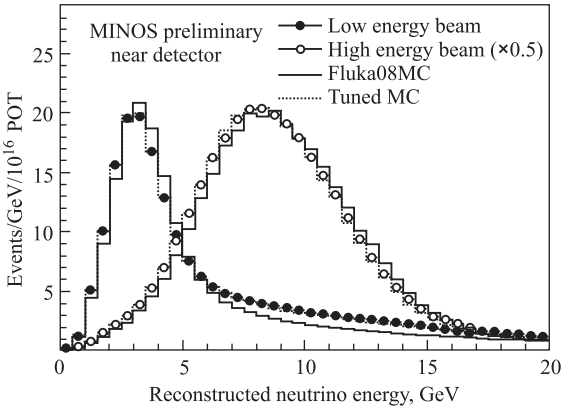

Fig. 6. Observed CC rates in the MINOS experiment for low and high energy configurations. Superimposed are MC predictions before and after tuning

segmentation and the same average magnetic field which allows significant cancellation of systematics due to uncertainties in neutrino cross sections and nuclear effects.

The NuMI beam spectra at the Near Detector, for both the low and high energy beam configurations are shown in Fig. 6. The data represent the ν_μ CC interaction rates and are compared both to the original FLUKA predictions, used as the starting point for the spectrum fit, and the final Monte Carlo prediction after adjustment of the hadronic production parameters. This observed near detector spectrum, extrapolated to the far detector using the best fit Monte Carlo, is shown in Fig. 7, *a* together with the actual data. There is clearly an energy-dependent deficit, shown quantitatively in Fig. 7, *b*, where we plot the ratio of observed to predicted CC rates as a function of the observed neutrino energy. The data are fitted to three hypotheses: two-flavor oscillation, pure decay and pure decoherence. The oscillation hypothesis gives an excellent fit to the data, whereas the other two hypotheses are disfavored at a level of 6.8 and 8.8 σ, respectively.

MINOS best fit parameters ($\Delta m^2_{13} = 2.35{\cdot}10^{-3}$ eV^2 and $\sin^2(2\theta_{23}) < 0.9$) as well as the 68 and 90% confidence level (CL) contours are displayed in Fig. 8 [7]. They are also compared with the latest Super-Kamiokande results [8, 9] from 2 different analyses for these parameters and the original 90% contour from the K2K experiment. Clearly the consistency of all results is very good; MINOS does better than Super-K on the Δm^2_{13} determination, but Super-K is able to set better limits on the value of the mixing angle. One should point out that the extraction of Δm^2_{13} in these two experiments uses very different methods and hence the systematics are quite different.

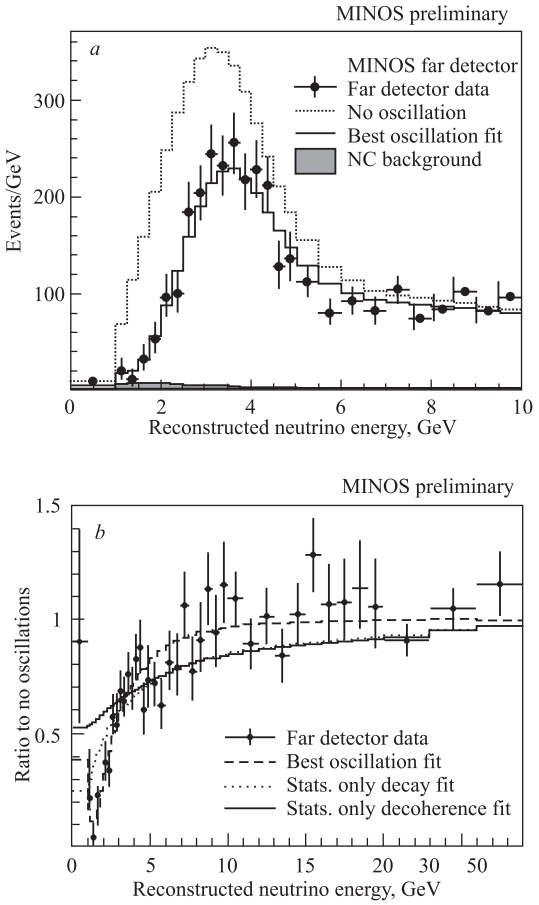

Fig. 7. *a*) MINOS CC ν_μ measured energy spectrum with superimposed no-oscillation and best fit oscillation predictions. *b*) Ratio of observed to no-oscillation predicted spectra. Superimposed are the predictions for three different disappearance hypotheses

These analyses, both from Super-K and MINOS, demonstrate that ν_μs disappear via oscillations but they do not explicitly determine the disappearance mode. Any significant conversion into ν_es is excluded by Super-Kamiokande, by the reactor experiment CHOOZ and by MINOS (as discussed below). Furthermore, the potential fraction of ν_μs that might be turning into $\nu_{\rm sterile}$ is also known to be relatively small. Accordingly there is strong indirect evidence that the neutrinos into which ν_μs oscillate are ν_τs.

The OPERA experiment has been designed to verify this hypothesis by direct detection of ν_τs. It uses a neutrino beam from CERN SPS protons and a specially

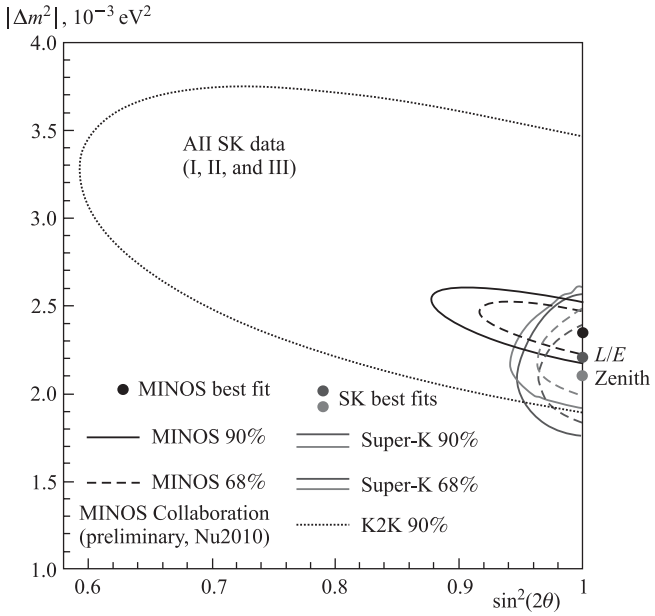

Fig. 8. The allowed oscillation parameters contour for the MINOS experiment together with the contours from other experiments

designed detector in the Gran Sasso Laboratory, 730 km away [10]. The detector uses bricks composed of emulsion and thin lead sheet layers which provide fine enough resolution to see the production and decay of tau leptons. In addition there are interspersed muon spectrometers composed of drift tubes, RPCs and magnets. These provide electronic information about approximate location of a potential neutrino interaction of interest and allow momentum measurement of the muon from the interaction. The energy of the beam is optimized to find the best compromise between the oscillation probability, neutrino flux, and ν_τ cross section. The resulting accepted spectrum is relatively flat between 8 and 25 GeV neutrino energy. The expected numbers of detected events for each τ decay mode, assuming a 5 year run with $4.5 \cdot 10^{19}$ POT/y are shown in Table 1, together with the expected background. The experiment is currently in the data taking phase and has recently reported the first potential observation of a ν_τ interaction followed by τ decay via $\tau^- \to \pi^- + \pi^0 + \nu_\tau$ mode. This candidate event is shown in Fig. 9 [11]. For the exposure used the expected background for this 1-prong topology is (0.018 ± 0.007) events giving a 1.8% probability that the event is due to background. The corresponding numbers for all topologies are (0.045 ± 0.023) events and 4.5% probability.

Table 1. **Projected signal and background event rates for a 5 year OPERA run for detected ν_τ decays produced via $\nu_\mu \to \nu_\tau$ oscillation**

Decay channel	Detection efficiency, %	Branching ratio, %	Signal	Background
$\tau \to \mu$	17.5	17.7	2.9	0.17
$\tau \to e$	20.8	17.8	3.5	0.17
$\tau \to h$	5.8	49.5	3.1	0.24
$\tau \to 3h$	6.3	15	0.9	0.17
All	eff $\times$ BR $= 10.6$		10.4	0.75

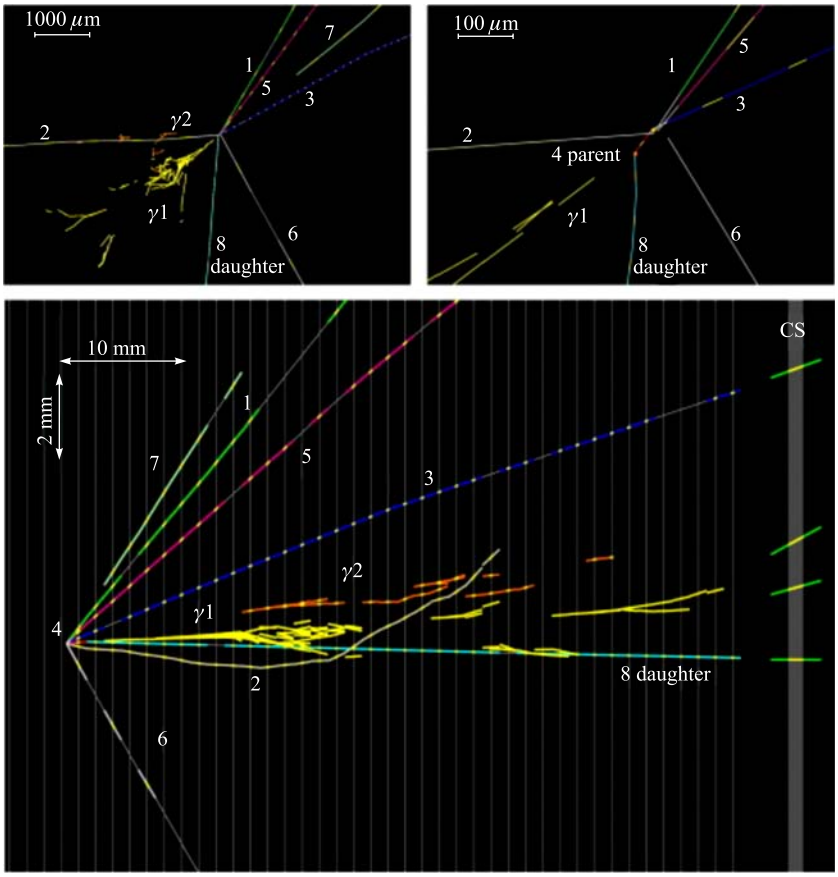

Fig. 9. A candidate ν_τ interaction event showing the subsequent τ decay into π^-, π^0, and ν_τ

3. STUDIES OF $\sin^2(2\theta_{13})$

So far, there have been three distinct approaches to determine the value of θ_{13}. The first one is the search for disappearance of $\overline{\nu}_e$s originating in a reactor. This method is conceptually very straightforward as it involves solely comparison of flux at a distant detector with the relatively well understood flux produced by the reactor and proportional to the reactor thermal power output. Furthermore, the interpretation is straightforward in so far that the size of the effect depends only on θ_{13}. But the measurement involves subtracting two large numbers and thus not only requires high statistics but also good understanding of all possible systematics. The most accurate measurement to date comes from the CHOOZ experiment which observed no disappearance and set the limit (assuming MINOS best value for Δm^2_{13} of $2.35 \cdot 10^{-3}$ eV^2) of $\theta_{13} < 11.5^\circ$ [12].

Alternatively, one can do three flavor analyses of different experiments, specifically experiments on solar neutrinos, Super-Kamiokande atmospheric data and KamLAND long baseline reactor experiment. Several theoretical and experimental groups have performed such analyses [13] and the results provide a mild suggestion for a small but nonzero θ_{13}. Needless to say, such studies require thorough understanding of all potential experimental biases and systematic uncertainties.

The third general method involves search for $\nu_\mu \to \nu_e$ transitions in accelerator experiments with a relatively pure ν_μ beam. The first such experiment was K2K which gave a limit $\sin^2(2\theta_{13}) < 0.22$ [14]. This transition to ν_es depends on several other parameters besides θ_{13}; the principal ones being θ_{23}, the CP phase δ, mass hierarchy (normal or inverted). This is both an advantage and disadvantage; advantage, because it gives you a handle on other important parameters; disadvantage because detailed interpretation of the results depends on the measurements from other experiments.

MINOS experiment has used its data to extract information on $\nu_\mu \to \nu_e$ transition [14]. While the ν_μ CC events are very easy to identify in the MINOS detector by the presence of a long muon track, the same is not true of the ν_e CC events. The relatively coarse MINOS granularity does not allow one to separate cleanly and unambiguously the electron induced electromagnetic shower from the rest of the neutrino interaction induced activity. The identification of the ν_e events has to be done on a statistical basis. These events tend to be skinnier and shorter than the typical neutral current (NC) interactions which provide the main background source. The other two most significant sources of the $\nu_\mu \to \nu_e$ background are high y ν_μ CC events and the ν_e events in the beam, primarily from muon decays. The ν_e separation is done by defining a number of topological variables that have a distribution that is significantly different for the NC and high y ν_μ events from those for the ν_e events. The analysis proceeds by defining a neural network based on 11 such topological variables. The network

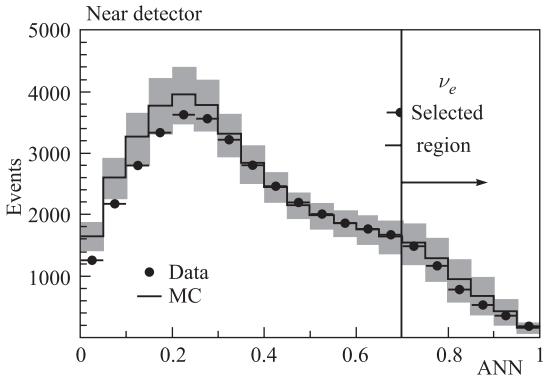

Fig. 10. The observed near detector neural network parameter for the ν_e candidates. Superimposed is the MC prediction

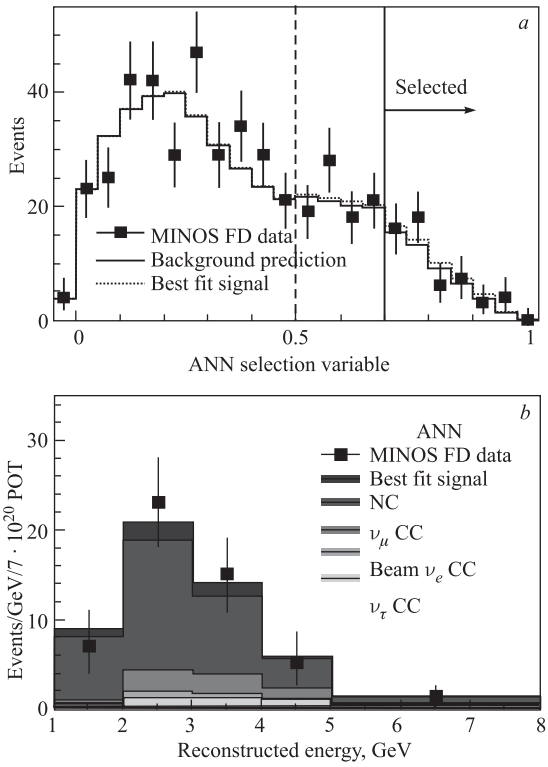

Fig. 11. *a*) Distribution of the ANN variable for the FD events passing the ν_e cuts. *b*) The energy spectrum of those data and of the calculated backgrounds, extrapolated from the data

outputs a single number between 0 and 1, with a low number indicating most probably a background event; and high number, a ν_e event. The ND data, which do not contain any oscillation ν_e events are used to optimize the neural network and find the optimum cut to separate the signal from the background. These data are displayed in Fig. 10 where we show data points superimposed on Monte Carlo prediction together with the adopted cut value. Extrapolation of these background sources to the Far Detector predicts (49.1 ± 7.0) background events where is included a small contribution from τ decays obtained from a Monte Carlo calculation. The ANN variable is plotted in Fig. 11 both for the background prediction and for the actual data. The 54 events are observed to the right of the cut, i.e., in the signal region. The small excess in the signal region can be interpreted as a (statistically not significant) signal or can be used to set a 90% CL limit on $\nu_\mu \to \nu_e$ oscillation. These results are indicated in Fig. 12, where we show it for the two mass hierarchies assuming in the calcula-

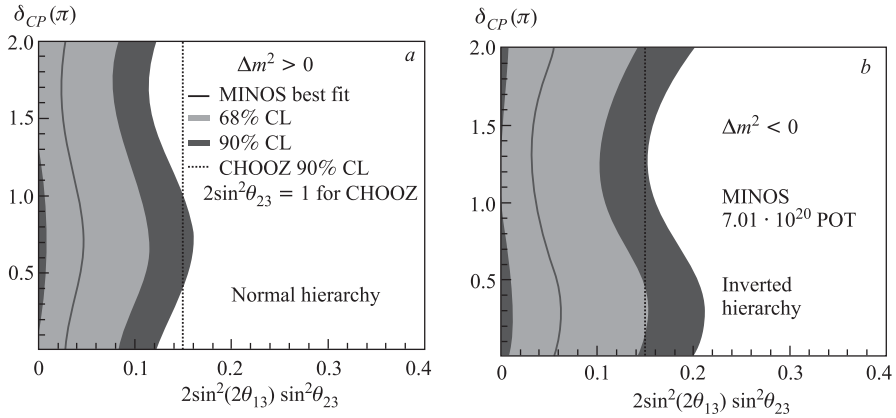

Fig. 12. MINOS allowed regions in the CP δ. $\sin^2\theta_{23}\sin^2(2\theta_{13})$ space

Table 2. **Compendium of results on $\sin^2(\theta_{13})$ from the currently available experiments and combined analyses**

Oscillation analysis	$\sin^2\theta_{13}$ (value)	$\sin^2\theta_{13}$ (90% CL)	$\sin^2\theta_{13}$ (95% CL)
Super-K (atm, norm)	$0.006^{+.030}_{-.006}$	< 0.066	
Super-K (atm, inv)	$0.044^{+.041}_{-.032}$	< 0.122	
Super-K (solar, global)	$0.025^{+.018}_{-.016}$		< 0.059
SNO (solar, global)	$0.020^{+.021}_{-.016}$		< 0.057
MINOS (norm) at $\delta_{CP} = 0$	$0.007^{+.014}_{-.007}$	< 0.03	
MINOS (inv) at $\delta_{CP} = 0$	$0.015^{+.021}_{-.013}$	< 0.05	
CHOOZ		< 0.037	

tions $\delta = 0$. In Table 2 we display the results for $\sin^2(\theta_{13})$ from different analyses together with the CHOOZ limit. All the results are consistent with that limit but they all give a slightly positive value. This compendium, even though not very significant, suggests a nonzero but small (~ 0.02) value for $\sin^2(\theta_{13})$. Note that in this compendium there is no factor of 2 in the argument of the sine function.

4. APPARENT ANOMALIES

In this section, I want to discuss a few experimental results which do not appear to fit into the standard picture of neutrino oscillations. The first of these is the long standing LSND (acronym for Liquid Scintillator Neutrino Detector) anomaly, stemming from an observation of $\overline{\nu}_e$ events in a situation where they should not have been produced originally [15]. The experiment was performed at the Los Alamos Laboratory and involved targeting the primary proton beam on a water target followed by a dense beam dump. The shielding between the target station and the detector ensured that the only significant flux arriving at the detector would be neutrinos. Their dominant source would be π^+ or μ^+ decays. The number of neutrinos from π^- and μ^- decays would be strongly suppressed by the fact that water target strongly favored π^+ production and any π^- produced would be much more likely to stop and be captured rather than decay. Thus, such an experimental situation would give predominantly ν_μ (from π^+ decays) and $\overline{\nu}_\mu$ and ν_e from μ^+ decays. The $\overline{\nu}_e$s would be absent in this scenario.

The experiment looked for possible transformation of $\overline{\nu}_\mu$ into $\overline{\nu}_e$. The signature for $\overline{\nu}_e$ interaction on proton would be detection of the prompt positron from the initial interaction followed by a delayed signal from the neutron capture in liquid scintillator. As is seen in Fig. 13, there was an apparent excess of detected $\overline{\nu}_\mu$s above what one would expect from potential sources such as π^- decays in flight, cosmic rays, accidental coincidences, etc. The background sources could be either directly measured or calculated from other measurements.

The $\overline{\nu}_e$ excess could be interpreted as oscillation of $\overline{\nu}_\mu$s into $\overline{\nu}_e$s. The possible oscillation parameters which can explain this result are illustrated in Fig. 14. All possible values would require Δm^2 which is significantly higher than the two which explain the solar and atmospheric neutrino phenomena. Thus, this would require the fourth neutrino mass state. The only way to reconcile that with the Z° decay result, which showed that there are only three light neutrinos, is to postulate that the fourth neutrino would be sterile, i.e., have no Standard Model interactions.

MiniBooNE experiment was designed to test the LSND result under quite different conditions. An effort was made to cover roughly the same L/E range but the values of both L and E were about an order of magnitude larger. The experiment uses the 8 GeV proton beam from the Fermilab Booster to produce

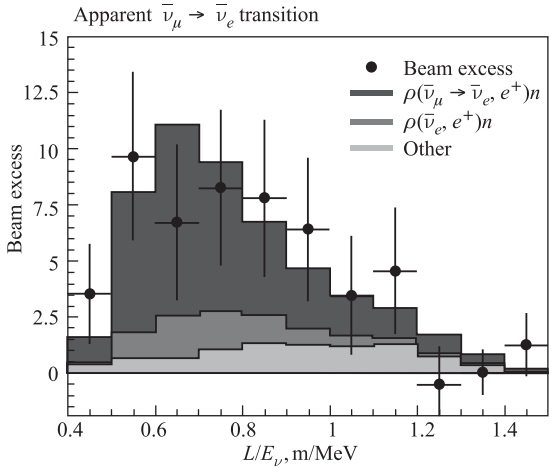

Fig. 13. L/E_ν distribution of the candidate $\overline{\nu}_e$ events in the LSND experiment. The calculated contributions from the different sources are indicated

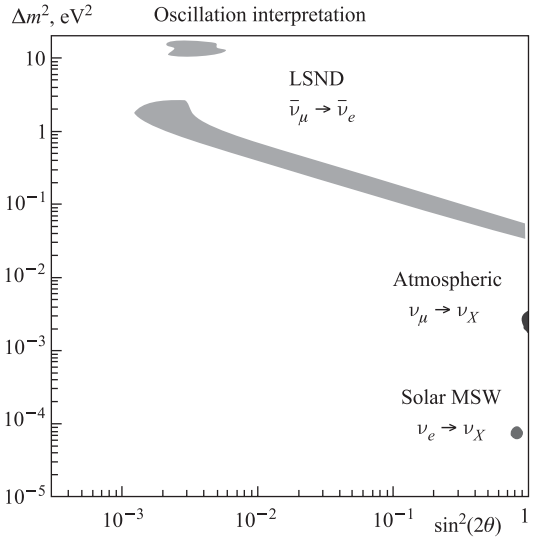

Fig. 14. The region in the oscillation parameters space allowed by the LSND data if the $\overline{\nu}_e$ excess is interpreted as oscillations

the neutrino beam and the detector is similar in its basic nature to the LSND one. It consists of a tank filled with approximately 800 t of mineral oil and lined with photomultipliers recycled from the LSND experiment. The optical signal consists

of Cherenkov light and small amount of scintillator light. The target is inside the magnetic horn whose polarity can be changed to focus either positive or negative secondaries. The drift distance for pion decays is 50 m and is followed by about 500 m of the earth absorber both to stop the muons and to provide potential path length for the oscillations. There is only one (far) detector which is covered with about 3 m of earth overburden to cut out most of the hadronic and electromagnetic component in the cosmic rays and reduce the muon flux by about the factor of 2.

The neutrino beam is mainly ν_μs or $\overline{\nu}_\mu$s depending on the horn polarity. The signal would be ν_es or $\overline{\nu}_e$s, produced by transformation of the muonic component. Thus the experiment faces similar challenges as MINOS in extracting a small ν_e (or $\overline{\nu}_e$) signal in the presence of both NC interactions and beam ν_es. The identification of the signal is also done based on topology even though clearly the variables used here are quite different. Since there is no near detector, one has to rely to a greater extent on Monte Carlo simulations and use of the actual data to generate input necessary for accurate prediction of the background.

The experiment has already taken $6.5 \cdot 10^{20}$ protons on target (POT) with the neutrino beam [16] and is currently running with antineutrinos. To date $5.7 \cdot 10^{20}$ POT have been analyzed from this second data set [17]. The neutrino (antineutrino) energy spectra for events passing all the ν_e ($\overline{\nu}_e$) cuts for the quasieleastic hypothesis are displayed in Fig. 15, *a* and *b*, for neutrinos and antineutrinos, respectively. The contributions to the background from different sources are also indicated showing that the background is dominated by the misidentified π^0s and beam ν_es. In Fig. 15, *a* and *b*, is indicated the region corresponding to the LSND observation of an anomalous signal. There appears to be no excess of events in that region for the neutrino case but there is an excess at energies below the LSND region. The excess could be due to either electrons or gamma rays since the detector cannot distinguish between these two hypotheses. In contrast,

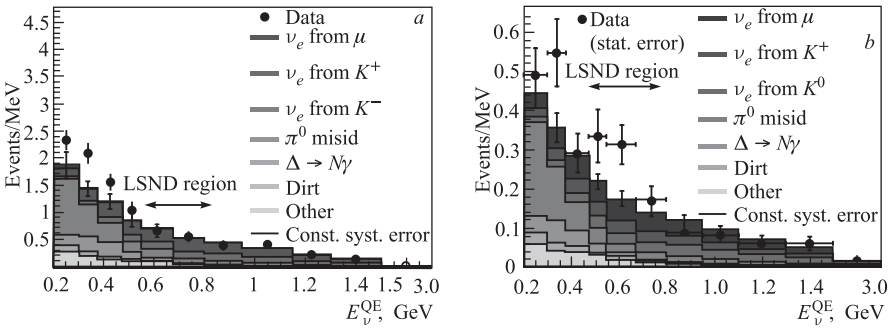

Fig. 15. The observed energy spectra of the candidate ν_e (*a*) and $\overline{\nu}_e$ (*b*) events in the MiniBooNE experiment together with the calculated contributions from the different background sources

the antineutrino data shows an excess of signal events in the LSND region but much smaller excess at low energies, consistent with being due to the neutrino component in the beam. The magnitude of the excess in the antineutrino data in the LSND-relevant energies is consistent with what one would expect from the observed signal in that original experiment.

Various efforts have been made to explain these (and the LSND) data in terms of existence of sterile neutrino(s). Single sterile neutrino appears insufficient to explain all of these data and at least two sterile neutrinos seem to be necessary [18]. The MiniBooNE experiment is in the process of taking more antineutrino data to improve the statistical accuracy of this measurement.

MINOS has performed a search for sterile neutrinos but in a different region of parameter space than investigated by LSND and MiniBooNE. Those experiments are sensitive in the large Δm^2 but small mixing angle domain. On the other hand, MINOS can look in the atmospheric region, i.e., small Δm^2 and relatively large mixing angle [19]. It can thus provide limits on the fraction of ν_μs that might be oscillating into sterile neutrinos. In the conventional picture there should be no depletion of neutral current events since that process does not distinguish between flavors. Thus, MINOS experimental procedure is to look for deficiency of the NC events in the far detector. The specific procedure follows the same path as the CC disappearance analysis. First, NC events are identified in the near detector by the absence of a muon, appearing as a long rack. Subsequently this measurement is used to predict the NC rate in the far detector using the energy-dependent Monte Carlo ratio of far to near detector rates for both the NC signal and the backgrounds.

The spectrum of visible energy for events passing the NC selection cuts, together with the MC prediction, is displayed in Fig. 16. There is a reasonably large uncertainty on the MC prediction, mainly due to the unknowns in the nuclear interaction model. This uncertainty, however, does not affect very much the near/far ratio because of strong correlations in the two detectors and hence the resultant cancellation. The main background, as can be seen from Fig. 16, is the CC background, representing high y events, where the muon is too short to be identified with high level of accuracy. The ν_e CC events would be generally classified as the NC events and thus the interpretation of the results depends on the assumption one makes about the value of θ_{13}.

Figure 17 shows the far detector data together with the prediction based on the near detector measurement. This prediction is shown both for the null value of θ_{13} and for $\theta_{13} = 11.5°$, i.e., the CHOOZ limit. There is no evidence for any depletion of the NC event with respect to the prediction. Quantitatively, we expect to see 757 events (signal + background) assuming no $\nu_\mu \to \nu_e$ conversion and observe 802. We can define

$$R = (N_{\rm data} - N_{\rm bkd})/{\rm signal}_{\rm MC}. \tag{3}$$

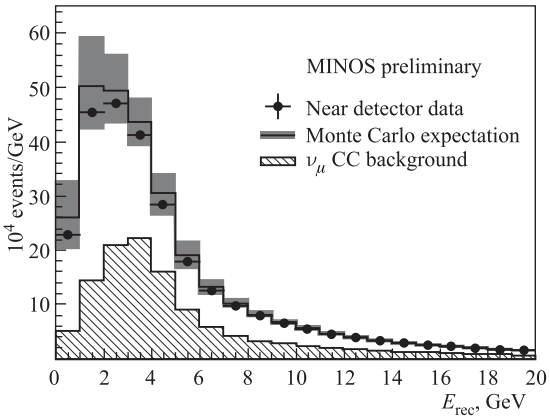

Fig. 16. Energy spectrum of MINOS NC candidate events in the near detector together with the MC calculated expected spectrum and the calculated CC background contribution

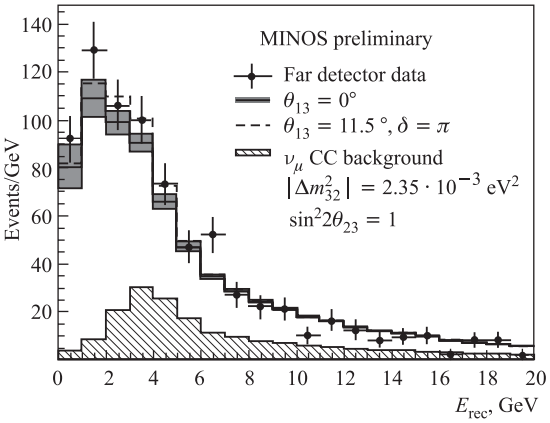

Fig. 17. Energy spectrum of MINOS NC candidate events in the far detector together with the expected spectrum extrapolated from the near detector and with the calculated CC background contribution

Then $R = 1.09 \pm 0.06(\text{stat.}) \pm 0.05(\text{syst.})$. For the fraction of ν_μs which oscillate into sterile neutrinos, defined as

$$f_{st} = \frac{P(\nu_\mu \to \nu_{\rm sterile})}{(1 - P(\nu_\mu \to \nu_\mu))}, \tag{4}$$

we obtain $f_{st} = 0.22(0.40)$ at 90% CL where the number in parentheses corresponds to $\theta_{13} = 11.5°$.

Another potentially very interesting and anomalous result is the measurement of the oscillation parameters by MINOS for $\overline{\nu}_\mu$s [20]. This is the first such measurement in an accelerator produced beam configured to preferentially accept $\overline{\nu}_\mu$s. Both the polarity of the magnetic horns and the direction of the magnetic field in the two detectors have been reversed with respect to the original neutrino configuration. Due to the differences in cross sections and in hadronic production, both of them are favoring neutrinos, the fraction of neutrinos in the antineutrino tuned beam is higher than the reverse situation for a neutrino beam. This is illustrated in Fig. 18. Because of this, more stringent cuts on the muon charge determination have been used in this analysis so as to reduce that potential background in the final event sample. Presence of magnetic field is clearly necessary if one wants to identify antineutrino events on an event-by-event basis.

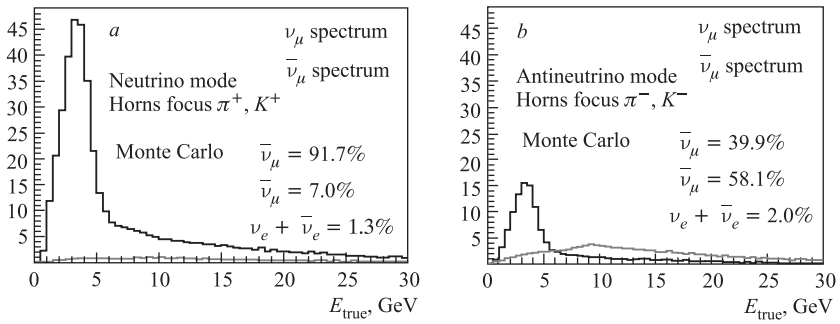

Fig. 18. ν_μ and $\overline{\nu}_\mu$ spectra for the neutrino tuned beam (*a*) and the antineutrino tuned beam (*b*)

The basic analysis procedure is very similar to that used for the neutrino analysis. Near detector data are used to make a prediction as to what one should see in the far detector under different oscillation hypotheses. Likelihood function is then minimized to give the best fit parameters. The muon antineutrino energy spectrum in the far detector for the currently analyzed exposure of $1.7 \cdot 10^{20}$ POT is shown in Fig. 19 together with the prediction from the near detector both on the assumption of no oscillations and for the best fit. The best fit parameters are $\Delta m^2 = 3.36 \cdot 10^{-3}$ eV^2 and $\sin^2(2\theta_{23}) = 0.86 \pm 0.11$. The contours in the 2-dimensional space for both neutrinos and antineutrinos are displayed in Fig. 20. The probability that both sets of data are governed by the same parameters is at a level of 2.3σ.

MINOS is in the process of continuing the antineutrino run with a goal of achieving a total exposure of $4 \cdot 10^{20}$ POT. Clearly, if this result holds up with increased statistics, it would indicate some new physics, either anomalous interaction that is different for neutrinos and antineutrinos [21] or violation of

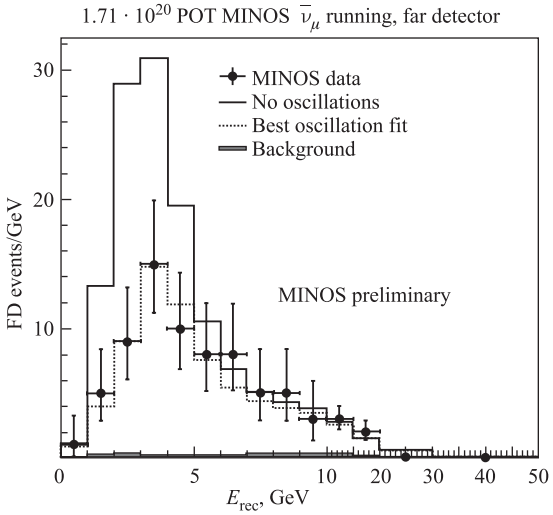

Fig. 19. MINOS CC $\overline{\nu}_\mu$ observed energy spectrum in an antineutrino tuned beam with superimposed no-oscillation and best fit oscillation predictions

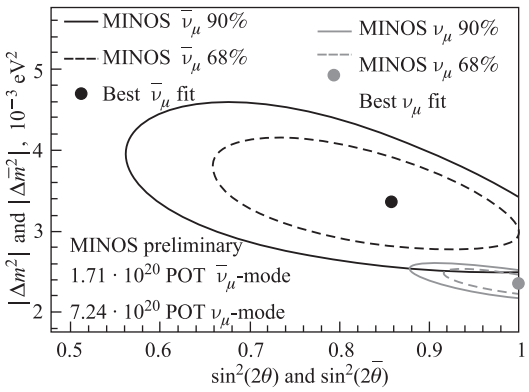

Fig. 20. Allowed contour in the oscillation parameter space for the $\overline{\nu}_\mu$ exposure together with a similar contour for the ν_μ experiment

fundamental symmetries. Parenthetically one should point out that the hypothesis of equal oscillation parameters in the solar sector has not been tested very well. This is because the solar experiments, using neutrinos, constrain the mixing angle very well but the mass squared difference rather poorly. The opposite situation holds true for KamLAND which is observing neutrinos.

5. FUTURE ACCELERATOR EFFORTS (NEAR TERM)

Before discussing future experiments it is useful to summarize the current status of our knowledge of neutrino oscillation in the framework of the standard model of neutrino oscillations. Of the seven parameters describing the oscillations: the three mixing angles, two mass squared differences, CP phase, and the mass hierarchy, four are quite well known today, namely θ_{12} and θ_{23} and the two Δm^2s. Thus the focus of the future experiments is the determination of the other three, initially θ_{13} and then CP phase and mass hierarchy. So far, there is only a limit on θ_{13} (as discussed earlier) but nothing is known about the other two.

There are two near term accelerator efforts designed to address these questions. The first of these is the T2K experiment in Japan [22]. It uses a new neutrino beam based on the extracted protons from the recently constructed JPARC accelerator facility. The beam is aimed at the Super-Kamiokande detector 295 km away. The data taking has already started in 2010 but at a significantly lower intensity than the design value. Significant increase in intensity is anticipated for the forthcoming run.

The other effort is the NOvA experiment based at Fermilab [23]. It will use the NuMI beam line but look at the beam at an off-axis angle. The detector will be brand new and will be located on the surface in Ash River, MN, 810 miles from Fermilab. It is a 14 t, highly segmented liquid scintillator detector with 80% of its mass being active. The detector is currently under construction with the start of data taking with a partial detector scheduled for the latter part of 2012.

The basic goals of both experiments are very similar and focused initially on observation of the $\nu_\mu \to \nu_e$ transition and thus obtaining new information on θ_{13}. Both experiments use off-axis beams optimized for maximum flux near the center of the atmospheric oscillation peak. Because the distances from target location to detectors are quite different in the two cases, the neutrino energy chosen for the T2K experiment is much lower, peaking around 800 MeV, to be compared with the NOvA peak energy around 2.5 GeV. The significantly longer distance used by NOvA gives it some sensitivity to determination of mass hierarchy if θ_{13} is in the range being suggested by some experimental results (as discussed previously).

The layout of the T2K neutrino beam line is shown in Fig. 21. There are three detectors: INGRID is an on-axis detector whose function is to monitor the beam by looking at the muons from neutrino parents. The so-called ND280 detector is an electronic detector, located 280 m from the target, and is designed to study the neutrino interactions in some detail and be able to identify exclusive channels. It will provide detailed input to the Monte Carlo simulations for the far detector, the Super-Kamiokande. Both the ND280 and Super-K are positioned off-axis at 2.5°. The resulting beam at that angle is shown in Fig. 22 which also illustrates the advantage of off-axis configuration when one wants to obtain a reasonably monochromatic beam.

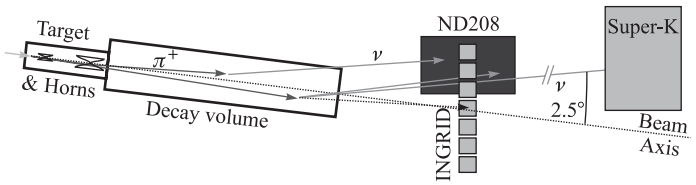

Fig. 21. Schematic of the beam line in the T2K experiment

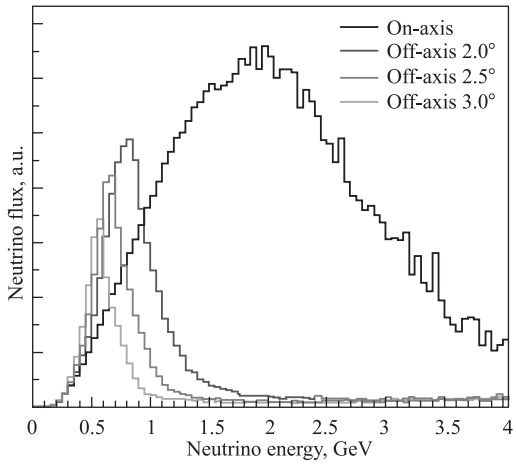

Fig. 22. Neutrino energy spectra from the T2K beam line for the on-axis configuration and various off-axis possibilities

The initial run at the beginning of 2010 was performed at 50 kW, significantly less than the design value of 750 kW. A number of beam upgrades are planned for the next couple of years with a goal of achieving that design value. Probably the most important of these is the increase of the proton linac injector energy. The primary goal of T2K is measurement of θ_{13}. The sensitivity reach of the experiment for a 5 year run at the design intensity is shown in Fig. 23. The sensitivity has a strong dependence on the value of CP parameter δ as can be seen in the Figure but only weak dependence on the mass hierarchy because of the relatively low energy used. The experiment should also be able to improve our knowledge of the oscillation parameters in the atmospheric sector. The advertised values for the full 5 year run are 10^{-4} eV^2 uncertainty on Δm^2 and ability to see deviations from unity of $\sin^2(2\theta_{23})$ up to 0.99.

The NOvA experiment plans to use a novel detector composed entirely of plastic rectangular tubes filled with liquid scintillator. The dimensions of the

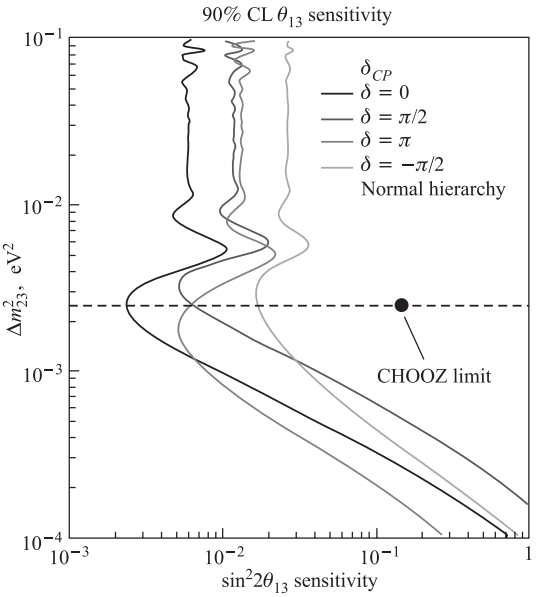

Fig. 23. Sensitivity of the T2K experiment for $\sin^2(2\theta_{13})$ as a function of Δm^2_{23} shown for several values of CP phase δ

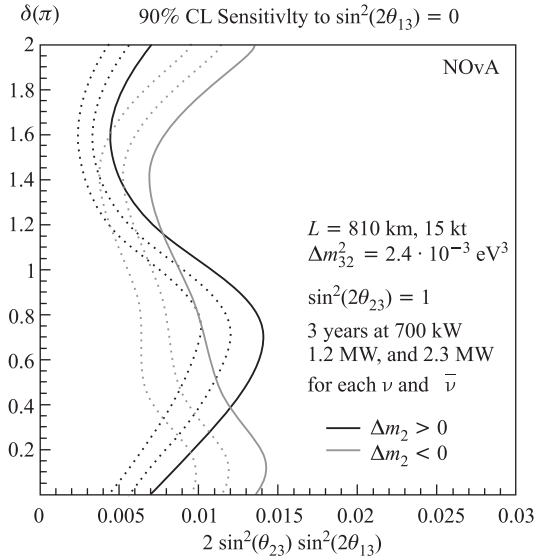

Fig. 24. NOvA sensitivity to $\sin^2\theta_{23}\sin^2(2\theta_{13})$ as a function of CP phase δ for both mass hierarchies and 3 different beam power values. A 3 year run for both neutrinos and antineutrinos is assumed

tubes are 15.7 m long, 4 cm wide and 6 cm deep (along beam direction). That granularity gives longitudinal sampling of $0.2X_0$; a 2 GeV muon will traverse 60 planes. The readout is done by a wavelength shifting fiber that is looped at one end of the cell; at the other end both fiber ends are connected to an APD. The ν_e events will be identified by the presence of an electromagnetic shower

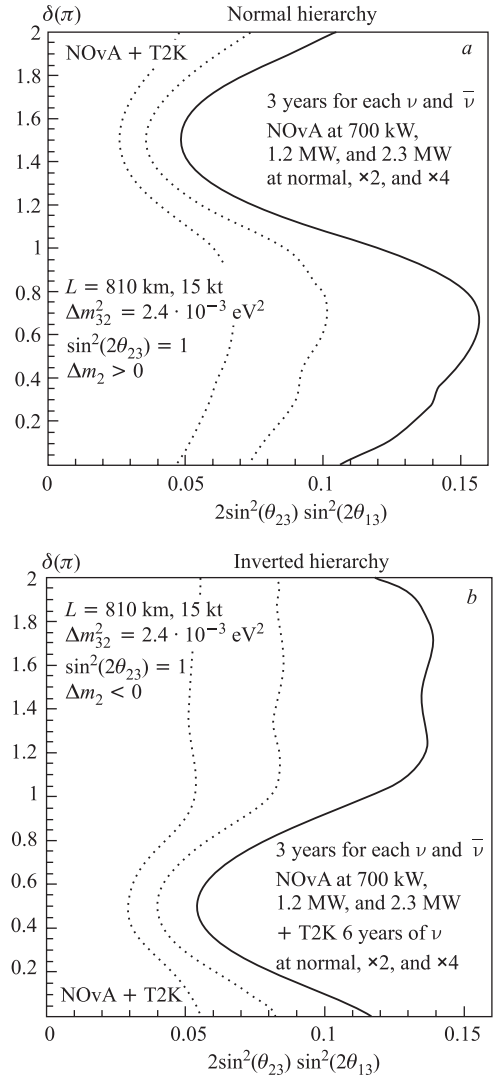

Fig. 25. Sensitivity of the combined data from the NOvA and T2K experiments for the determination of the mass hierarchy

along the electron track, i.e., relatively narrow band of energy deposition but one that extends over several neighboring cells. The total tonnage of the detector is 14 kt; its total length 67 m.

There will also be a near detector which is essentially a smaller replica of the main detector except that it will have iron plates at the back to range out all the muons in the interesting energy range. It will be located in the NuMI tunnel, about 1 km from the target. A prototype of its active part has been assembled on the surface and is currently taking data from the NuMI beam running antineutrinos. Its current location corresponds to a 110 mr off-axis angle with respect to the NuMI beam line.

The far detector is on a green site in Ash River, MN, so the experiment required significant site preparation before its construction could begin. The most important part of that phase is now complete and assembly of the detector should begin before the end of 2011. The detector is 810 km from the target, 14 mrad off-axis from the NuMI beam line. The NuMI beam line will be tuned to medium energy and the resulting spectrum in this configuration will be peaked around 2.5 GeV. As in the T2K experiment, the high energy neutrino flux will be strongly suppressed improving significantly signal to background ratio. The current plans for NOvA contemplate a 3 year run on neutrinos and a 3 year run on antineutrinos with beam power of 700 kW. The sensitivity to the mixing angle is displayed in Fig. 24. The ability to distinguish between the two mass hierarchies can be enhanced by doing a joint analysis of both the NOvA and T2K data sets. The fact that T2K is relatively insensitive to the mass hierarchy allows such an analysis to resolve some of the intrinsic ambiguities. The reach for mass hierarchy determination is shown in Fig. 25.

6. FUTURE PLANS (LONG TERM)

The current plans for programs beyond T2K and NOvA are still not very well defined. On a shorter time scale they involve significant upgrades to accelerators, neutrino beam lines, and detectors with a goal to significantly increase neutrino event rates. On a longer time scale there is an active research and development program around the world to develop new accelerator facilities like neutrino factories and beta beams. Discussion of these plans is beyond the scope of this report but a short review of the more immediate plans seems appropriate.

At this time, the future US program appears to be somewhat better defined than those in Asia and Europe. It is centered around eventual development of two new major facilities: a new underground laboratory and a new accelerator complex at Fermilab. The underground laboratory is the Deep Underground Science and Engineering Laboratory (DUSEL) to be developed at the former Homestake mine in Lead, South Dakota. The new accelerator facility is referred

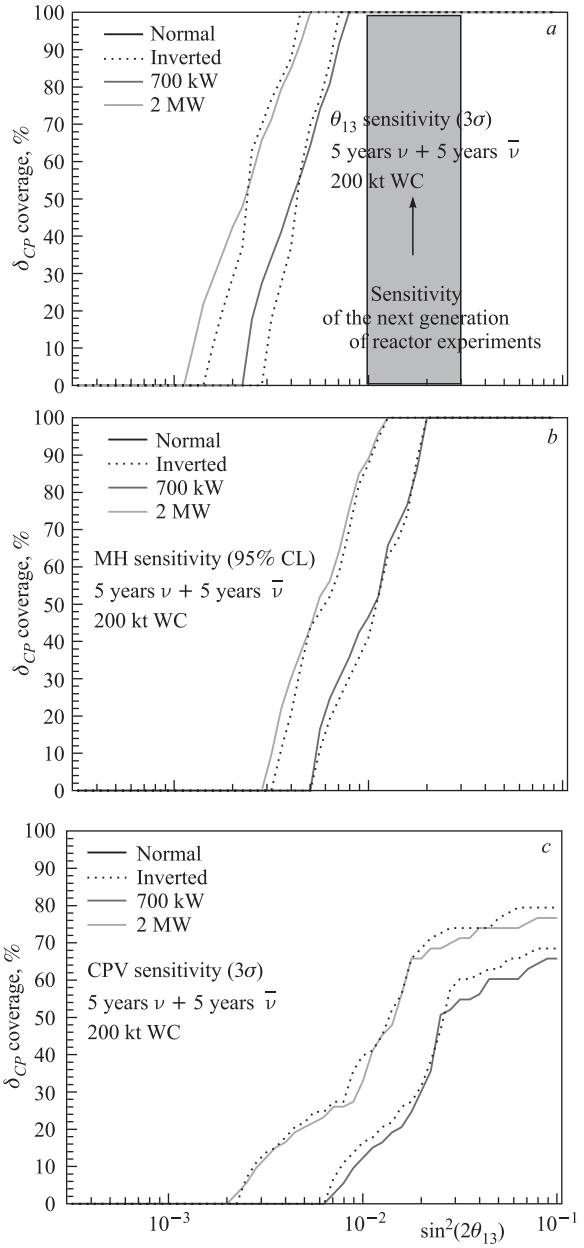

Fig. 26. Sensitivity of the LBNE experiment for detection of nonzero $\sin^2(2\theta_{13})$, for determination of the mass hierarchy and for observation of CP violation

to as Project X. It is a major upgrade of the Fermilab Main Injector achieved by replacement of the current 8 GeV Booster by an 8 GeV superconducting linac. Neither project is funded as of this date but the hope is that DUSEL project can be completed before the end of this decade and the Project X a few years later.

The first phase of this program would be the Long Baseline Neutrino Experiment (LBNE). It would require a new neutrino beam line aimed at DUSEL, about 1365 km away. Initially the beam would be operated at 700 kW but would be designed with a possibility of upgrade to an eventual power of 2 MW, expected to become feasible with the Project X.

The initial detector would be either a 100 kt fiducial mass water Cherenkov detector or an equivalent (about 17 kt) liquid argon detector. The laboratory would be designed so that additional detectors could be added later. The potential sensitivities for $\sin^2(\theta_{13})$, determination of mass hierarchy, and significant observation of CP violation are shown for two different beam intensities in Fig. 26.

The long range program in Asia is centered around an upgrade of the JPARC accelerator to 2.5 MW. Furthermore, the current beamline would be used in association with a new detector (or detectors) in the 0.5–1 Mt range. Several location/detector options are being considered ranging from a single large water Cherenkov detector near the current Super-K site to a large liquid argon detector on the island of Okinoshima, 658 km from the neutrino source, or two detectors separated by about 1000 km, one at the current Super-K site and the other one in Korea. Even though both water and liquid argon detectors are being considered, the water Cherenkov detector seems to be the preferred option today.

European long range plans in neutrino physics are even more uncertain mainly due to the fact that over the past few years the main focus there has been the LHC issues. There has been an ongoing study as to the best course to pursue and this work is supposed to be completed in 2011. In parallel there is going on an evaluation of seven potential sites for an underground laboratory.

7. CROSS SECTIONS

In the past, the major focus of neutrino cross section experiments has been studies of structure functions and measuring the fundamental parameters of the Standard Model. Today, the emphasis has shifted more towards investigations of intranuclear processes and providing important input for the oscillation experiments besides studying some fundamental processes like quasielastic scattering and coherent pion production. As discussed earlier, measurement of neutrino cross sections is difficult because of problematic issues associated with the determination of neutrino flux. Furthermore, the relative coarseness of most neutrino detectors makes studies of exclusive reactions and their properties difficult.

In principle, at least determination of the neutrino flux can be made in one of three ways. Production of hadrons can be measured in auxiliary experiments and the neutrino flux deduced from those results and from the beam geometry and focusing arrangements. Alternatively, flux can be determined by measuring the rate for a process whose cross section is known reliably from theory [24]. Finally, one can measure the flux of the decay muons. All of these methods have been tried in the past but none of them is easy. The existing problems with flux normalization are shown in the two graphics in Fig. 27, the plot *a* showing the measured quasielastic cross sections by different experiments, the plot *b* the

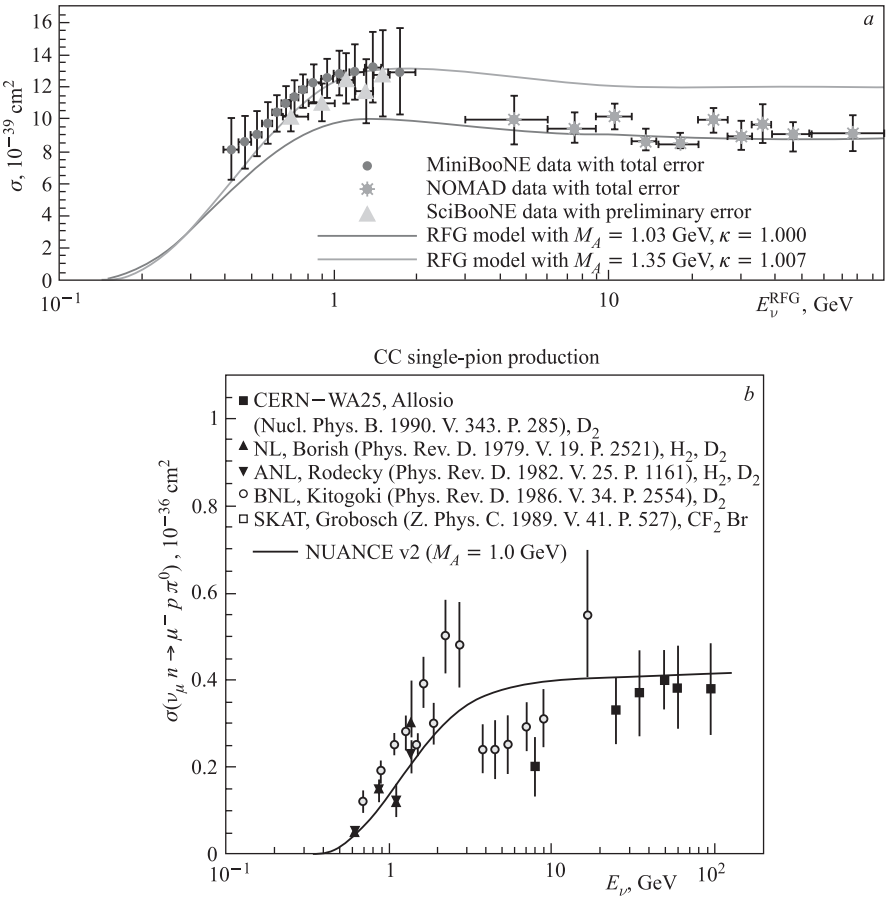

Fig. 27. Currently available data on the quasielastic ν_μ cross section (*a*) and on inclusive π^0 production (*b*)

inclusive pion production in the CC interactions. The lack of continuity in the data points to some uncertainty in the normalization of different experiments.

Today some progress is being made in the cross section studies by virtue of high statistics data samples in the near detectors of MINOS [24] and K2K [25], experiments with close by detectors like MiniBooNE [26] and dedicated cross section experiments like SciBooNE [27] and MINERvA [28]. Space does not allow me to discuss properly the results from these experiments. The current overall situation for total CC cross sections is shown in Fig. 28, where the older data points are augmented by the recent MINOS measurement.

Detailed understanding of some processes can be helped by the knowledge of exclusive reactions. Thus, for example, determination of $\nu_\mu \to \nu_e$ rate relies at some level on accurate determination of the background. More specifically,

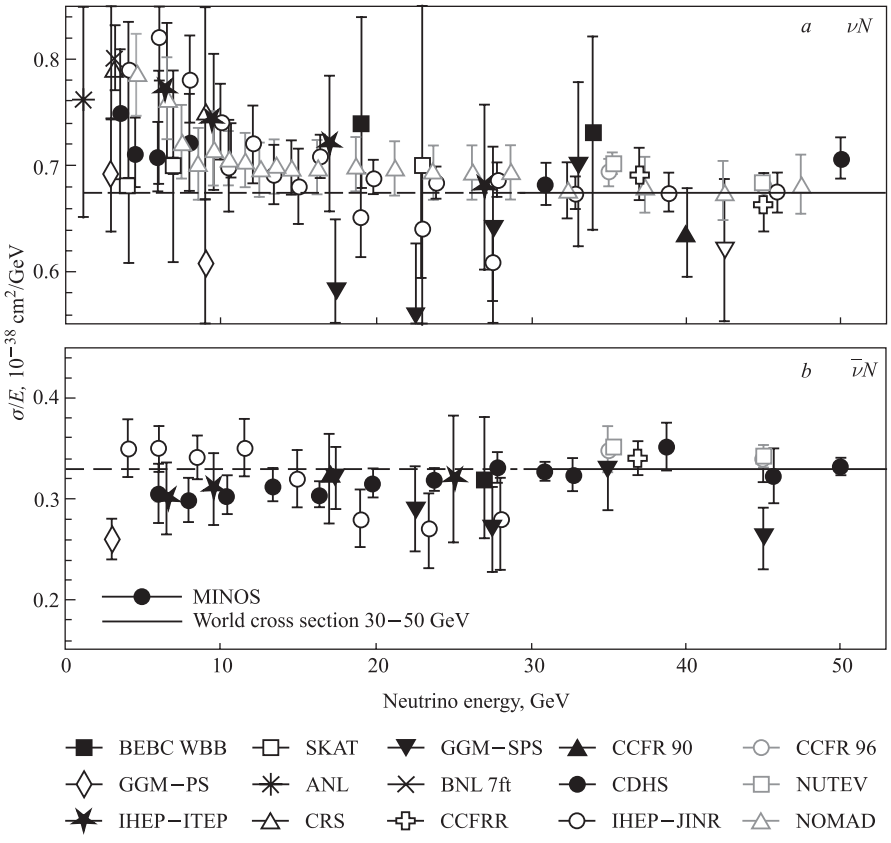

Fig. 28. Currently available data on the total CC ν_μ (*a*) and $\overline{\nu}_\mu$ (*b*) inclusive cross sections

it helps to know the rate and details for such reactions as resonance production and inclusive π^0 production, the chief source of background for this transition mode. The current knowledge, which forms an important input to the simulation programs, is rather poor. This is illustrated in Fig. 29 where we show the prediction from the NUANCE code regarding the invariant cross sections for the isobar production as a function of its mass and for the inclusive charged current π^0 production as a function of its momentum together with the results from the MiniBooNE experiment [29].

In the near future, we can look forward to rather detailed data in the medium energy range from the MINERvA experiment and from the ND280 near detector in T2K. Both of these are very fine grained detectors that will be exposed to very

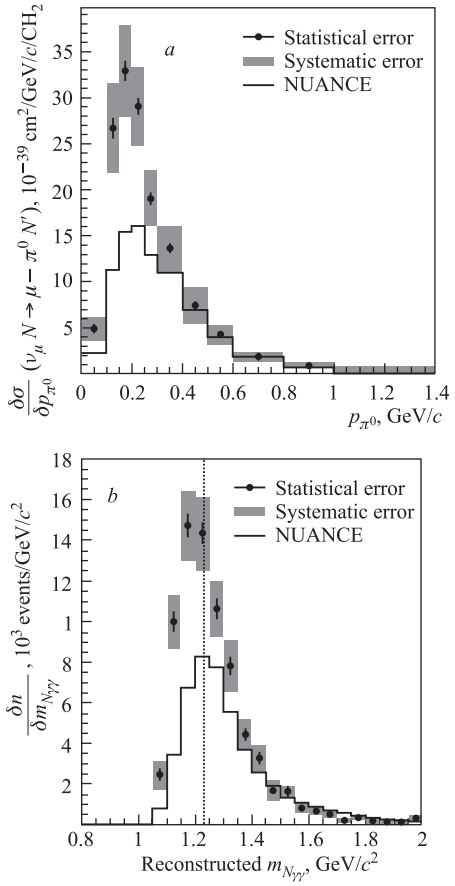

Fig. 29. Comparison of the NUANCE predictions with the MiniBooNE data for π^0 production (*a*) and production of nucleon-π system (*b*)

intense neutrino flux. Thus they should be able to provide detailed information on many exclusive channels of interest. ND280 would be sensitive mainly to the neutrino energies in the sub-GeV range whereas MINERvA would explore mainly the few GeV region.

8. SUMMARY

Over the last 12 years, since the discovery of neutrino oscillations in 1998, a great progress has been made in understanding that phenomenon. But a number of key questions are still awaiting answers. The accelerator based neutrino experiments have provided important and extensive information in these studies in the past. There is no doubt that they will continue to do so in the future. The technical advances in detectors, neutrino beams and in accelerators have played important role in advancing the capabilities of these experiments and will certainly continue to do so.

REFERENCES

1. *Pontecorvo B.* // JETP. 1959. V. 37. P. 1751.
2. *Schwartz M.* // Phys. Rev. Lett. 1960. V. 4. P. 306.
3. *Danby G. et al.* // Phys. Rev. Lett. 1962. V. 9. P. 36.
4. *Ahn M. H. et al. (K2K Collab.)* // Phys. Rev. D. 2006. V. 74. P. 072002.
5. *Adamson P. et al. (MINOS Collab.)* // Phys. Rev. D. 2008. V. 77. P. 072002.
6. *Michael D. et al. (MINOS Collab.)* // Nucl. Instr. Meth. A. 2008. V. 596. P. 190.
7. *Adamson P. et al. (MINOS Collab.)* // Phys. Rev. Lett. 2010. V. 283. P. 367.
8. *Ashie Y. et al. (SuperKamiokande Collab.)* // Phys. Rev. Lett. 2004. V. 93. P. 10181.
9. *Ashie Y. et al. (SuperKamiokande Collab.)* // Phys. Rev. Lett. 2005. V. 71. P. 112005.
10. *OPERA Collab.* // Nucl. Phys. Proc. Suppl. 2007. V. 168. P. 173;
Guler M. et al. (OPERA Collab.). CERN SPSC. 2001-025.
11. *Agafonova N. et al. (OPERA Collab.)* // Phys. Lett. B. 2010. V. 691. P. 138.
12. *Apollonio M. et al. (CHOOZ Collab.)* // Eur. Phys. J. C. 2003. V. 27. P. 331.
13. *Fogli G. L. et al.* // Phys. Rev. Lett. 2008. V. 101. P. 141801;
Schwetz T., Tortola M., Valle J. W. F. // New J. Phys. 2008. V. 10. P. 113011.
14. *Adamson P. et al. (MINOS Collab.)* // Phys. Rev. Rapid Commun. D. 2010. V. 82. P. 051102.
15. *Aguilar A. et al. (LSND Collab.)* // Phys. Rev. D. 2001. V. 64. P. 112007.
16. *Aguilar-Arevalo A. A. et al. (MiniBooNE Collab.)* // Phys. Rev. Lett. 2009. V. 102. P. 101802.

17. *Aguilar-Arevalo A. A. et al. (MiniBooNE Collab.)* // Phys. Rev. Lett. 2010. V. 105. P. 181801.

18. *Karagiorgi G. et al.* // Phys. Rev. D. 2010. V. 80. P. 073001.

19. *Adamson P. et al. (MINOS Collab.)* // Ibid. V. 81. P. 052004.

20. *Vahle P. (for MINOS Collab.)*. Invited paper presented at the 2010 Neutrino Conference, Athens, Greece.

21. *Wolfenstein D. L.* // Phys. Rev. D. 1978. V. 17. P. 2369;
Valle J. W. F. // Phys. Lett. B. 1987. V. 199. P. 432;
Gonzalez-Garcia M. C. et al. // Phys. Rev. Lett. 1999. V. 82. P. 3202;
Friedland A., Lundardini C., Maltoni M. // Phys. Rev. D. 2004. V. 70. P. 111301.

22. *Ytow Y. et al. (T2K Collab.)*. hep-ex/0106019v1. 2001.

23. *Ayers D. et al. (NOvA Collab.).* hep-ex/0403053v1. 2005.

24. *Adamson P. et al. (MINOS Collab.)* // Phys. Rev. D. 2010. V. 81. P. 072002.

25. *Ahn M. H. et al. (K2K Collab.)* // Phys. Rev. D. 2006. V. 74. P. 072003;
Nakayama Y. et al. (K2K Collab.) // Phys. Lett. B. 2005. V. 619. P. 255;
Gran R. et al. (K2K Collab.) // Phys. Rev. D. 2006. V. 74. P. 052002.

26. *Aguilar-Arevalo A. A. et al. (MiniBooNE Collab.)* // Phys. Rev. Lett. 2007. V. 100. P. 032031.

27. *Kurimoto Y. et al. (SciBooNE Collab.)* // Phys. Rev. D. 2010. V. 81. P. 033004.

28. *Drakoulakos D et al. (MINERvA Collab.)*. hep-ex/0405002.

29. *Aguilar-Arevalo A. A. et al. (MiniBooNE Collab.)* // Phys. Rev. D (submitted); hep-ex/1010.3264. 2010.

ФИЗИКА ЭЛЕМЕНТАРНЫХ ЧАСТИЦ И АТОМНОГО ЯДРА
2011. Т. 42. ВЫП. 4

ACCELERATOR NEUTRINO PHYSICS — CURRENT STATUS AND FUTURE PROSPECTS

S. G. Wojcicki

Stanford University, Stanford, CA, USA

This review article describes the current status and future prospects of accelerator neutrino physics. The emphasis is on recent developments in the oscillation physics area, but there is also a limited discussion about the status of neutrino cross sections. The approach taken is pedagogical, and an effort is made to explain the basic techniques used in the accelerator studies of neutrino physics.

PACS: 14.60.Pq; 95.55.Vj

INTRODUCTION

The neutrinos are ubiquitous in nature. They are not only produced constantly in natural phenomena like the burning of the Sun, explosion of supernovas, decays of cosmic ray secondaries, and decays of radioactive elements in the air, on the Earth's surface and deep inside the Earth but also are believed to have been created some 13 billion years ago in the Big Bang. Furthermore, they can be produced in or by man-made sources: reactors, nuclear explosions, accelerators, and artificially produced radioactive isotopes.

Given the multiplicity of neutrino sources, it is not surprising that they cover a very broad energy spectrum, different sources being generally characterized by neutrinos of a characteristic spectrum and of different intensity. At one extreme are the cosmological neutrinos created in the Big Bang with present flux of about $10^{22}/(\mathrm{cm}^2 \cdot \mathrm{s} \cdot \mathrm{sr} \cdot \mathrm{MeV})$ and energies in the μeV to meV range. On the other extreme are the so-called GZK neutrinos with fluxes in the $10^{-26}/(\mathrm{cm}^2 \cdot \mathrm{s} \cdot \mathrm{sr} \cdot \mathrm{MeV})$ and energies in the PeV to EeV range. Our current knowledge of neutrino physics is based on a wide range of studies of neutrinos from different sources. This diversity of spectra and sources has allowed us to probe the nature of neutrinos in surprisingly great detail.

Accelerator experiments have played a very important role in developing our current understanding of neutrinos. This was due to the versatility and flexibility of neutrino accelerator experiments, the ability to control the flavor and energy of the neutrinos and, very importantly, many technological improvements in this general area. This paper will attempt to briefly map out this history and these features, describe the recent advances, and summarize the future prospects.

1. BASICS OF ACCELERATOR NEUTRINO EXPERIMENTS

The first ideas to use decays of pions produced in accelerators as the source of neutrinos was independently due to B. Pontecorvo [1] and M. Schwartz [2]. Pontecorvo focused on studying potential anomalies in ν_μ interactions while Schwartz saw this primarily as a way of studying weak interactions without any significant interference from the much stronger weak and strong forces. The first accelerator experiment which succeeded in observing neutrinos was the one at Brookhaven by the Columbia group which also was able to show that ν_μ and ν_e had different interactions and hence were distinct [3].

The Brookhaven experiment was quite primitive by the today's standards. The primary proton beam struck an internal target and no focusing was used. Accordingly the fluxes were relatively modest and there was no significant separation between neutrinos and antineutrinos. In the subsequent years, the two most important technical developments relevant for neutrino studies were invention and development of neutrino horns and mastery of clean extraction of the circulating proton beam. Neutrino horn, so called because of its typical horn-like shape, was basically a configuration of two conductors where a flow of electric current would generate toroidal magnetic field. Thus, depending on the direction of the current, either positive or negative particles would be focused (the others being defocused), and hence the resulting flux was predominantly either neutrinos or antineutrinos. The horns were pulsed in synchronism with the extracted beam with typical currents of around 200 kA. The ability to extract the proton beams enabled much better shielding and thus lowered irradiation of neighboring elements (and hence made higher intensities possible), allowed more flexibility in targeting and focusing, and gave possibility of producing parent meson beams at 0° with respect to the proton beam which further increased the overall neutrino intensities.

The standard and most frequently used neutrino beams, are produced from decays of pions and kaons, with the dominant two-body decays into π and ν_μ providing most of the flux. Neutrinos originating from K decays give a higher energy flux, their energies reaching close to the energy of the parent kaon; on the other hand, the neutrinos from pion decays are limited kinematically to at most 42% of the parent pion energy. An important additional component in standard beams are ν_es originating either from the three-body decays of the kaons (branching ratio about 5%) or from tertiary muon decays.

Even in the standard, horn focused beam, commonly referred to as a wide band beam, one can control to a certain extent the energy spectrum of the produced neutrinos. This is done by adjusting the longitudinal position of the target with respect to the first magnetic horn. Furthermore, the combination of that position and the value of the generated magnetic field determine the range of the production transverse momenta of the parents that are most effectively focused. As an

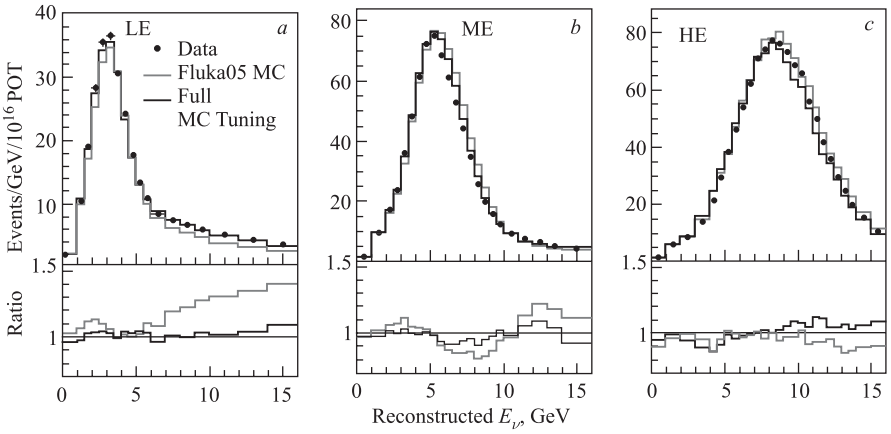

Fig. 1. NuMI CC event rates for different target locations: 10, 100, and 250 cm (corresponding roughly to the distance between the downstream end of the target and the point 20 cm upstream of the neck of the first horn) together with the MC predictions, before and after tuning. The data/MC ratios for these two MC predictions are indicated at the bottom

example, in Fig. 1 we show the energy spectrum of the NuMI beam at Fermilab for three different distances between the target and the first horn.

In the intervening time since the first neutrino experiment there were a number of other variations of the basic concept of neutrino beam that have been used in such experiments. Very briefly they were:

• Bare target beams, like the original BNL experiment. They allow somewhat cleaner determination of the neutrino flux since no focusing is involved but one pays penalty in the total intensity.

• Sign selected beam, where one uses a dipole to cleanly reject the parents of unwanted sign.

• Narrow band beam, where one selects the accepted momentum bite of the parent mesons.

• Beam dump «beam», where one tries to minimize as much as possible the available decay region for the parent mesons.

• Off-axis beam where the accepted neutrinos come off at a nonzero angle with respect to the initial proton (and accepted mesons) direction. Such an arrangement gives a rather narrow energy spectrum with an intensity at the chosen energy that is significantly higher than would be obtained in a wide band beam.

Determination of neutrino energy spectrum presents unique challenges that are not present in a typical charged particle beam or even neutral hadron beam.

In principle, the flux of neutrinos can be determined with the help of auxiliary experiment(s) which measures the production of hadrons by protons of the comparable energy to that used in the neutrino experiment. The resulting neutrino flux can then be derived using Monte Carlo simulations from those measurements, knowledge of the beam geometry and the properties of the focusing system.

In practice, however, that is quite difficult. The hadronic production experiments performed to date have suffered from inadequate statistics, lack of coverage of the complete required final-state phase space and/or somewhat different proton energies and target geometries, requiring additional complex extrapolations and simulations. The method that is generally adopted in long baseline neutrino experiments is to use two detectors, the first one relatively close to the target and the second one at a distance appropriate for the desired oscillation measurement. In this configuration, the near detector is used to measure the flux times cross section by observing the rate of (generally charged current — CC) interactions as a function of energy and then extrapolating those measurements to the far detector. Some Monte Carlo calculations are still needed to make this extrapolation but the level of the required knowledge of proper Monte Carlo input is relatively modest in this approach. Many of the uncertainties like those regarding detailed flux knowledge and energy dependence of cross sections cancel in this procedure.

There is some ambiguity as to the optimal features of the near detector. On the one hand, one wants the detector to be as similar in its internal construction as the far detector so as to eliminate or reduce most of the uncertainties inherent in the extrapolation. On the other hand, one also wants it to have the capability to measure the nature of the interactions in as detailed a way as possible. The ideal solution would be to have two near detectors, each one optimized for different

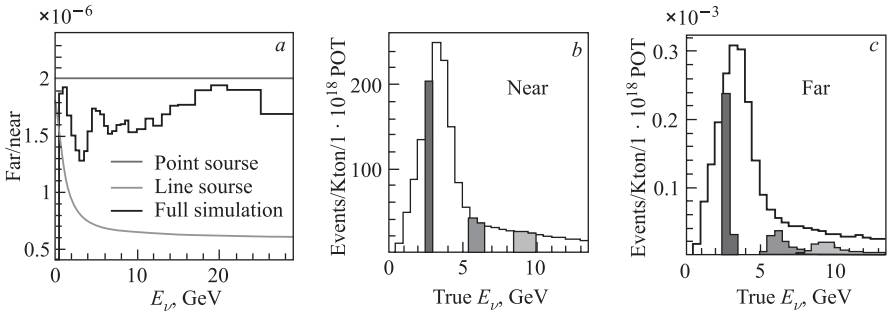

Fig. 2. Far/near ratio for the NuMI beam. *a*) These ratios for the actual case and for a line source and a point source. Plots *b* and *c* show how the different bands of neutrino energies in the near detector extrapolate to the far detector

function, but that is seldom adopted due to the pressures to keep low the total cost of the experiment. Different experiments constructed so far have adopted different solutions.

Figure 2 shows the details of the Near/Far extrapolation for the NuMI beam in the MINOS experiment. The relationship between the two is given by

$$N_{\mathrm{FD}}^{\mathrm{pred}} = (N_{\mathrm{FD}}^{\mathrm{MC}}/N_{\mathrm{ND}}^{\mathrm{MC}})N_{\mathrm{ND}}^{\mathrm{obs}}. \quad (1)$$

The ratio has an energy dependence which is illustrated in Fig. 2, *a* and is due to the fact that we have a line source for neutrinos and hence different acceptance ratio for the near detector depending on the point of decay. Plot *c* shows the far detector neutrino spectrum generated by the parent mesons giving neutrinos in a small energy band in the near detector as shown in Fig. 2, *b*.

2. STUDIES OF DOMINANT OSCILLATION PARAMETERS IN THE ATMOSPHERIC SECTOR

The neutrino oscillations in the atmospheric domain are dominated by two parameters, the mass squared difference, Δm^2_{13}, and mixing angle $\sin^2(2\theta_{23})$. Typical experiment looks for disappearance of ν_μs via detection of their CC interactions. The formula, in the two-flavor approximation, for the ν_μ survival probability, is given by

$$P(\nu_\mu \to \nu_\mu) = 1 - \sin^2(2\theta)\sin^2(1.27\Delta m^2 L/E). \quad (2)$$

The parameters are generally extracted by a simultaneous fit to both of them but different features of the energy spectrum tend to determine each one. The mass squared difference is determined principally by the location of the dip in the ratio of the observed to predicted number of events; the mixing angle is governed by the depth of this dip. This is illustrated in Fig. 3, where we have used arbitrary values of these two parameters, namely $\Delta m^2_{13} = 3.35 \cdot 10^{-3}$ eV^2 and mixing angle $\sin^2(2\theta_{23}) = 1$. The first long baseline neutrino experiment was the K2K in Japan where neutrinos were produced by a beam from the KEK 12 GeV proton synchrotron and detected by Super-Kamiokande water Cherenkov detector 225 km away [4]. There were two near detectors used. One of them was a smaller water Cherenkov counter, the other — a fine grained detector. The experiment suffered from low statistics but nevertheless was able to demonstrate energy-dependent disappearance of muon neutrinos which was consistent with the oscillation hypothesis with oscillation parameters in agreement with those measured by the Super-Kamiokande in its investigation of atmospheric neutrinos. The oscillation parameters were extracted independently both from the overall

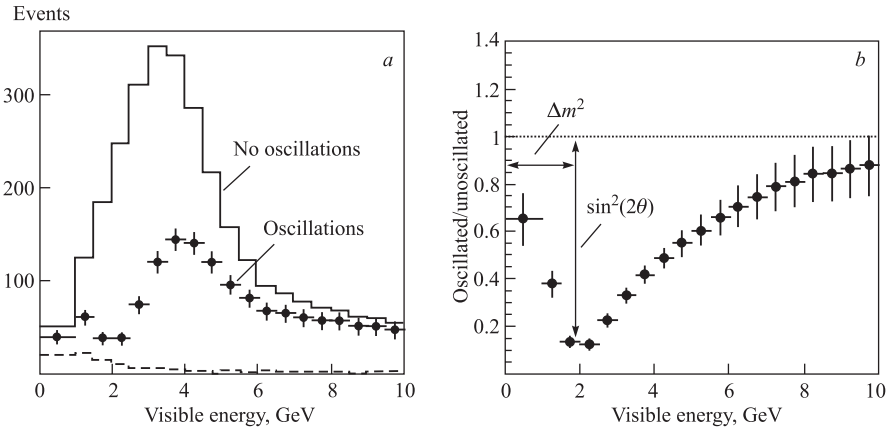

Fig. 3. An example of the effect of oscillations using MC calculations. The rates without and with oscillations are shown on the plot *a* and their ratio on the plot *b*. That figure also indicates the features of this ratio curve that mainly determine the oscillation parameters

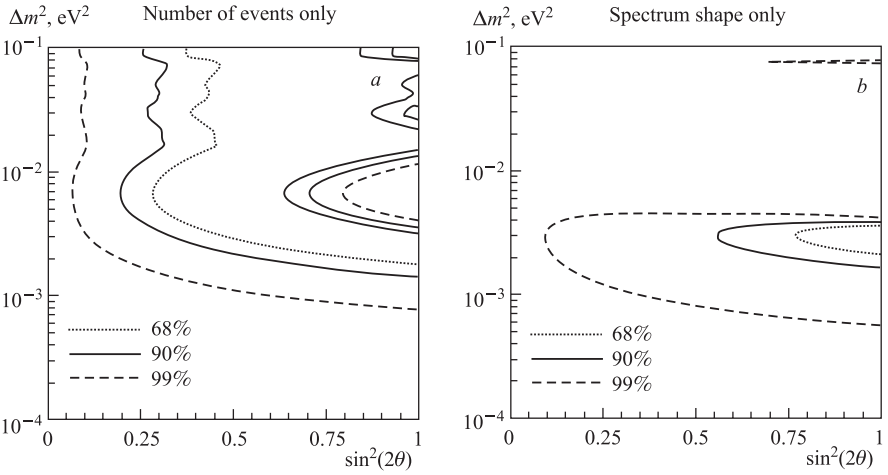

Fig. 4. The allowed oscillation parameter space for the K2K experiment obtained from the event rate only (*a*) and from the spectrum shape only (*b*)

CC event rate in the Super-Kamiokande and from shape-only spectrum, the latter providing better constraints as indicated in Fig. 4. The best measurement was obtained from the energy spectrum of 58 single ring ν_μ events as shown in Fig. 5.

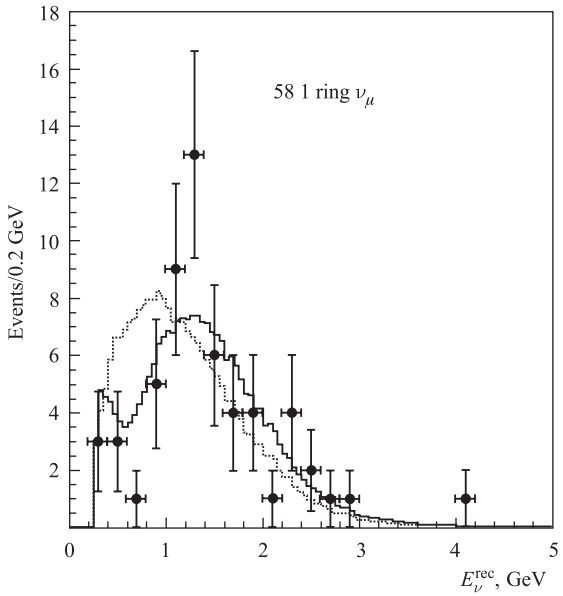

Fig. 5. The measured K2K spectrum using the 1 ring ν_μ events only. Superimposed are the best fits with oscillations (solid) and without oscillations (dotted)

MINOS experiment was designed for more detailed investigation of the atmospheric sector [5]. It uses the NuMI beam at Fermilab, produced by the 120 GeV protons from the Main Injector accelerator. The principal (far) detector of 5.4 kt is located in a former iron mine in Soudan, MN, at a distance of 725 km from the target. A smaller (near), 980 t detector is located 1.04 km from the target, at Fermilab, and serves to provide a detailed measurement of the neutrino flux at that site. The principal oscillation measurement is done with the beam tuned to low energy, peaking at about 3 GeV. Shorter runs at several different energies were made to obtain better constraints on the p_T and p_z distributions of the parent hadrons and thus better accuracy in extrapolating the neutrino spectrum to the far detector.

The experiment has been designed to optimize the measurement of the ν_μ disappearance via its charged current interactions [6]. Thus the design choice was to optimize the total tonnage at the expense of fine granularity. The detectors are iron scintillator calorimeters with a toroidal magnetic field averaging about 1.2 T. The general structure is alternating planes of iron, 2.5 cm thick, and scintillator planes composed of 4.1 cm wide strips whose orientation changes by 90° in successive planes. The two detectors have the same transverse and longitudinal

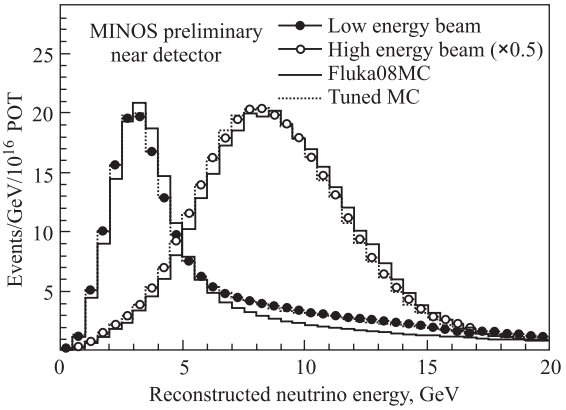

Fig. 6. Observed CC rates in the MINOS experiment for low and high energy configurations. Superimposed are MC predictions before and after tuning

segmentation and the same average magnetic field which allows significant cancellation of systematics due to uncertainties in neutrino cross sections and nuclear effects.

The NuMI beam spectra at the Near Detector, for both the low and high energy beam configurations are shown in Fig. 6. The data represent the ν_μ CC interaction rates and are compared both to the original FLUKA predictions, used as the starting point for the spectrum fit, and the final Monte Carlo prediction after adjustment of the hadronic production parameters. This observed near detector spectrum, extrapolated to the far detector using the best fit Monte Carlo, is shown in Fig. 7, *a* together with the actual data. There is clearly an energy-dependent deficit, shown quantitatively in Fig. 7, *b*, where we plot the ratio of observed to predicted CC rates as a function of the observed neutrino energy. The data are fitted to three hypotheses: two-flavor oscillation, pure decay and pure decoherence. The oscillation hypothesis gives an excellent fit to the data, whereas the other two hypotheses are disfavored at a level of 6.8 and 8.8 σ, respectively.

MINOS best fit parameters ($\Delta m^2_{13} = 2.35{\cdot}10^{-3}$ eV^2 and $\sin^2(2\theta_{23}) < 0.9$) as well as the 68 and 90% confidence level (CL) contours are displayed in Fig. 8 [7]. They are also compared with the latest Super-Kamiokande results [8, 9] from 2 different analyses for these parameters and the original 90% contour from the K2K experiment. Clearly the consistency of all results is very good; MINOS does better than Super-K on the Δm^2_{13} determination, but Super-K is able to set better limits on the value of the mixing angle. One should point out that the extraction of Δm^2_{13} in these two experiments uses very different methods and hence the systematics are quite different.

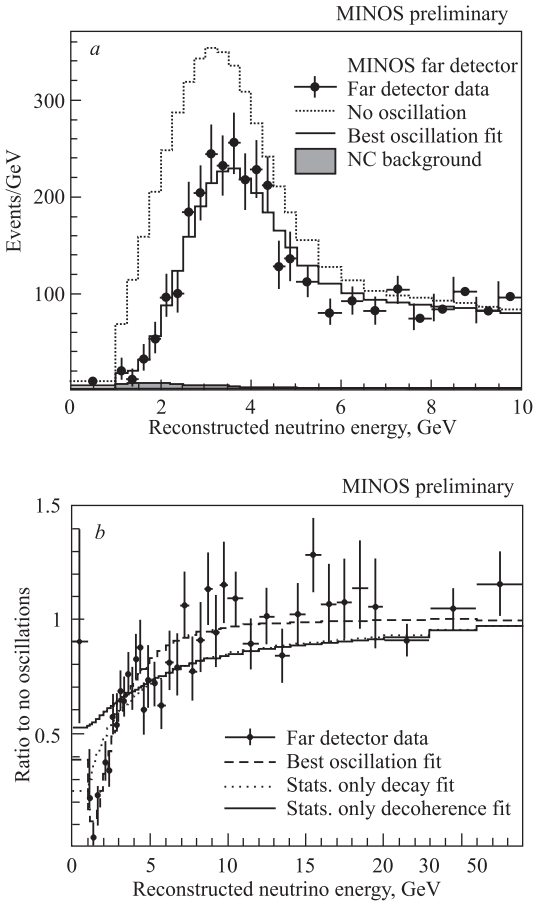

Fig. 7. *a*) MINOS CC ν_μ measured energy spectrum with superimposed no-oscillation and best fit oscillation predictions. *b*) Ratio of observed to no-oscillation predicted spectra. Superimposed are the predictions for three different disappearance hypotheses

These analyses, both from Super-K and MINOS, demonstrate that ν_μs disappear via oscillations but they do not explicitly determine the disappearance mode. Any significant conversion into ν_es is excluded by Super-Kamiokande, by the reactor experiment CHOOZ and by MINOS (as discussed below). Furthermore, the potential fraction of ν_μs that might be turning into $\nu_{\rm sterile}$ is also known to be relatively small. Accordingly there is strong indirect evidence that the neutrinos into which ν_μs oscillate are ν_τs.

The OPERA experiment has been designed to verify this hypothesis by direct detection of ν_τs. It uses a neutrino beam from CERN SPS protons and a specially

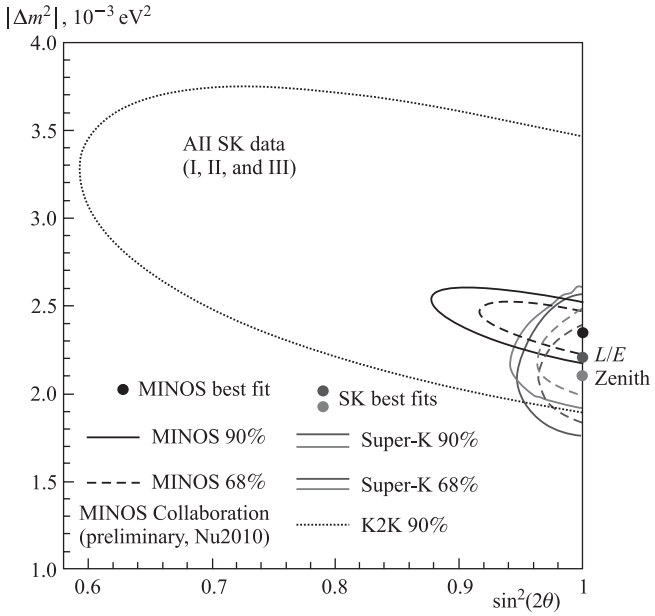

Fig. 8. The allowed oscillation parameters contour for the MINOS experiment together with the contours from other experiments

designed detector in the Gran Sasso Laboratory, 730 km away [10]. The detector uses bricks composed of emulsion and thin lead sheet layers which provide fine enough resolution to see the production and decay of tau leptons. In addition there are interspersed muon spectrometers composed of drift tubes, RPCs and magnets. These provide electronic information about approximate location of a potential neutrino interaction of interest and allow momentum measurement of the muon from the interaction. The energy of the beam is optimized to find the best compromise between the oscillation probability, neutrino flux, and ν_τ cross section. The resulting accepted spectrum is relatively flat between 8 and 25 GeV neutrino energy. The expected numbers of detected events for each τ decay mode, assuming a 5 year run with $4.5 \cdot 10^{19}$ POT/y are shown in Table 1, together with the expected background. The experiment is currently in the data taking phase and has recently reported the first potential observation of a ν_τ interaction followed by τ decay via $\tau^- \to \pi^- + \pi^0 + \nu_\tau$ mode. This candidate event is shown in Fig. 9 [11]. For the exposure used the expected background for this 1-prong topology is (0.018 ± 0.007) events giving a 1.8% probability that the event is due to background. The corresponding numbers for all topologies are (0.045 ± 0.023) events and 4.5% probability.

Table 1. **Projected signal and background event rates for a 5 year OPERA run for detected ν_τ decays produced via $\nu_\mu \to \nu_\tau$ oscillation**

Decay channel	Detection efficiency, %	Branching ratio, %	Signal	Background
$\tau \to \mu$	17.5	17.7	2.9	0.17
$\tau \to e$	20.8	17.8	3.5	0.17
$\tau \to h$	5.8	49.5	3.1	0.24
$\tau \to 3h$	6.3	15	0.9	0.17
All	eff $\times$ BR $= 10.6$		10.4	0.75

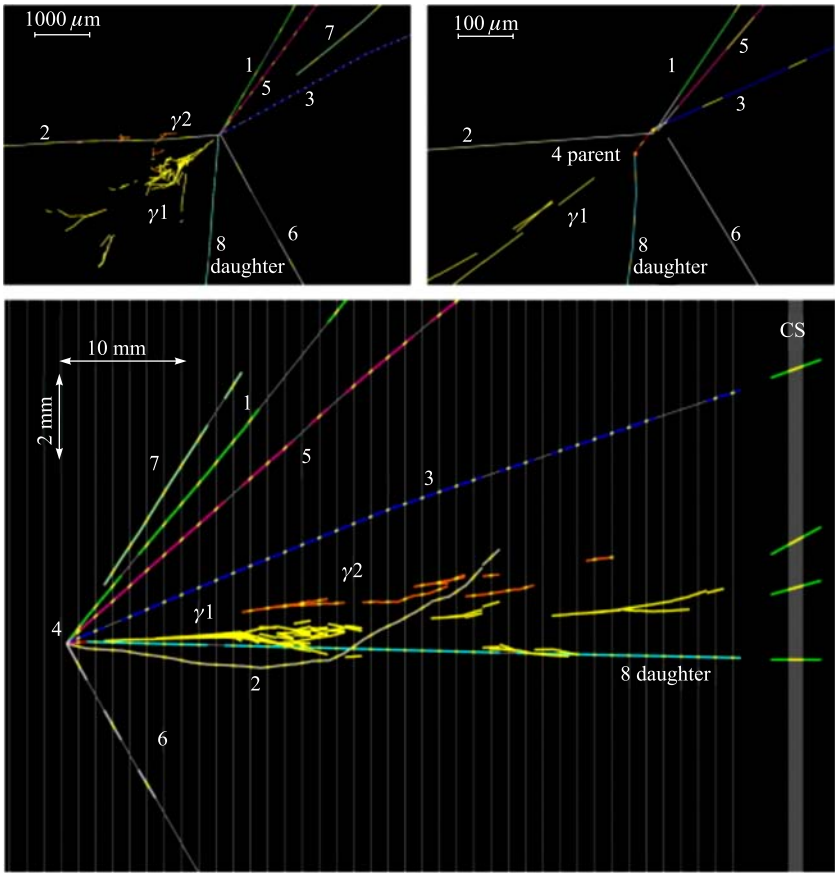

Fig. 9. A candidate ν_τ interaction event showing the subsequent τ decay into π^-, π^0, and ν_τ

3. STUDIES OF $\sin^2(2\theta_{13})$

So far, there have been three distinct approaches to determine the value of θ_{13}. The first one is the search for disappearance of $\overline{\nu}_e$s originating in a reactor. This method is conceptually very straightforward as it involves solely comparison of flux at a distant detector with the relatively well understood flux produced by the reactor and proportional to the reactor thermal power output. Furthermore, the interpretation is straightforward in so far that the size of the effect depends only on θ_{13}. But the measurement involves subtracting two large numbers and thus not only requires high statistics but also good understanding of all possible systematics. The most accurate measurement to date comes from the CHOOZ experiment which observed no disappearance and set the limit (assuming MINOS best value for Δm^2_{13} of $2.35 \cdot 10^{-3}$ eV^2) of $\theta_{13} < 11.5^\circ$ [12].

Alternatively, one can do three flavor analyses of different experiments, specifically experiments on solar neutrinos, Super-Kamiokande atmospheric data and KamLAND long baseline reactor experiment. Several theoretical and experimental groups have performed such analyses [13] and the results provide a mild suggestion for a small but nonzero θ_{13}. Needless to say, such studies require thorough understanding of all potential experimental biases and systematic uncertainties.

The third general method involves search for $\nu_\mu \to \nu_e$ transitions in accelerator experiments with a relatively pure ν_μ beam. The first such experiment was K2K which gave a limit $\sin^2(2\theta_{13}) < 0.22$ [14]. This transition to ν_es depends on several other parameters besides θ_{13}; the principal ones being θ_{23}, the CP phase δ, mass hierarchy (normal or inverted). This is both an advantage and disadvantage; advantage, because it gives you a handle on other important parameters; disadvantage because detailed interpretation of the results depends on the measurements from other experiments.

MINOS experiment has used its data to extract information on $\nu_\mu \to \nu_e$ transition [14]. While the ν_μ CC events are very easy to identify in the MINOS detector by the presence of a long muon track, the same is not true of the ν_e CC events. The relatively coarse MINOS granularity does not allow one to separate cleanly and unambiguously the electron induced electromagnetic shower from the rest of the neutrino interaction induced activity. The identification of the ν_e events has to be done on a statistical basis. These events tend to be skinnier and shorter than the typical neutral current (NC) interactions which provide the main background source. The other two most significant sources of the $\nu_\mu \to \nu_e$ background are high y ν_μ CC events and the ν_e events in the beam, primarily from muon decays. The ν_e separation is done by defining a number of topological variables that have a distribution that is significantly different for the NC and high y ν_μ events from those for the ν_e events. The analysis proceeds by defining a neural network based on 11 such topological variables. The network

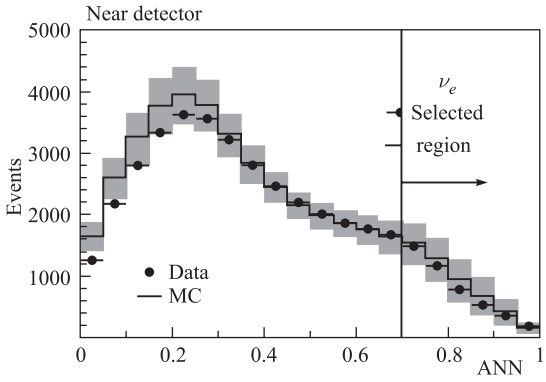

Fig. 10. The observed near detector neural network parameter for the ν_e candidates. Superimposed is the MC prediction

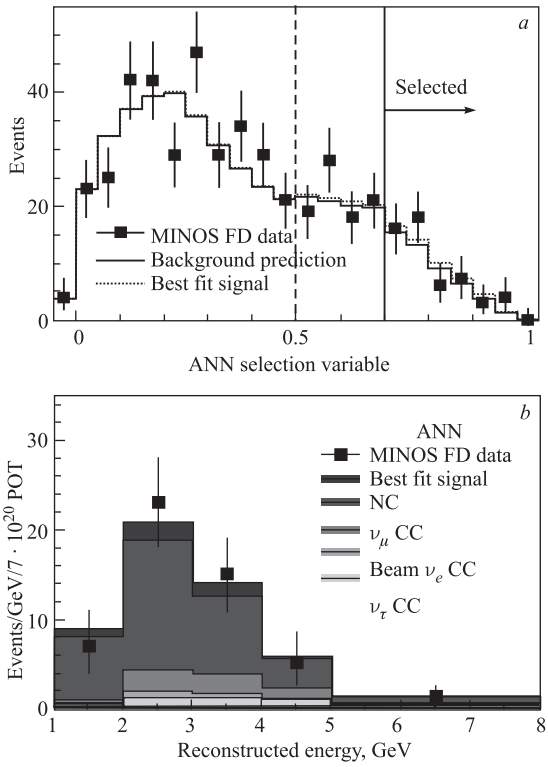

Fig. 11. *a*) Distribution of the ANN variable for the FD events passing the ν_e cuts. *b*) The energy spectrum of those data and of the calculated backgrounds, extrapolated from the data

outputs a single number between 0 and 1, with a low number indicating most probably a background event; and high number, a ν_e event. The ND data, which do not contain any oscillation ν_e events are used to optimize the neural network and find the optimum cut to separate the signal from the background. These data are displayed in Fig. 10 where we show data points superimposed on Monte Carlo prediction together with the adopted cut value. Extrapolation of these background sources to the Far Detector predicts (49.1 ± 7.0) background events where is included a small contribution from τ decays obtained from a Monte Carlo calculation. The ANN variable is plotted in Fig. 11 both for the background prediction and for the actual data. The 54 events are observed to the right of the cut, i.e., in the signal region. The small excess in the signal region can be interpreted as a (statistically not significant) signal or can be used to set a 90% CL limit on $\nu_\mu \to \nu_e$ oscillation. These results are indicated in Fig. 12, where we show it for the two mass hierarchies assuming in the calcula-

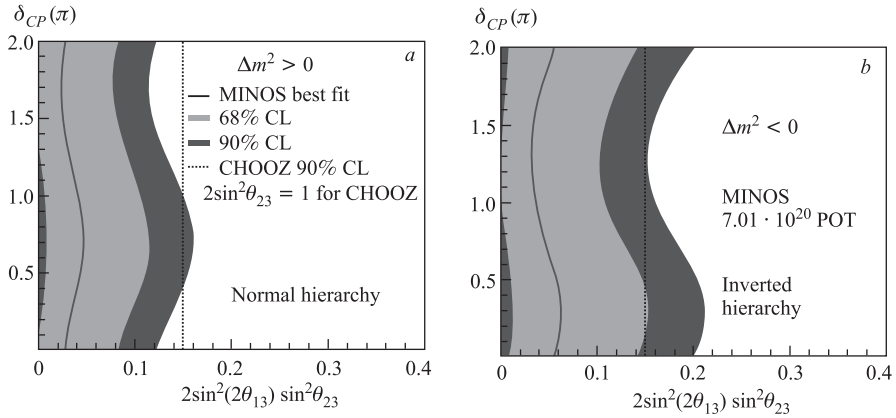

Fig. 12. MINOS allowed regions in the CP δ. $\sin^2\theta_{23}\sin^2(2\theta_{13})$ space

Table 2. **Compendium of results on $\sin^2(\theta_{13})$ from the currently available experiments and combined analyses**

Oscillation analysis	$\sin^2\theta_{13}$ (value)	$\sin^2\theta_{13}$ (90% CL)	$\sin^2\theta_{13}$ (95% CL)
Super-K (atm, norm)	$0.006^{+.030}_{-.006}$	< 0.066	
Super-K (atm, inv)	$0.044^{+.041}_{-.032}$	< 0.122	
Super-K (solar, global)	$0.025^{+.018}_{-.016}$		< 0.059
SNO (solar, global)	$0.020^{+.021}_{-.016}$		< 0.057
MINOS (norm) at $\delta_{CP} = 0$	$0.007^{+.014}_{-.007}$	< 0.03	
MINOS (inv) at $\delta_{CP} = 0$	$0.015^{+.021}_{-.013}$	< 0.05	
CHOOZ		< 0.037	

tions $\delta = 0$. In Table 2 we display the results for $\sin^2(\theta_{13})$ from different analyses together with the CHOOZ limit. All the results are consistent with that limit but they all give a slightly positive value. This compendium, even though not very significant, suggests a nonzero but small (~ 0.02) value for $\sin^2(\theta_{13})$. Note that in this compendium there is no factor of 2 in the argument of the sine function.

4. APPARENT ANOMALIES

In this section, I want to discuss a few experimental results which do not appear to fit into the standard picture of neutrino oscillations. The first of these is the long standing LSND (acronym for Liquid Scintillator Neutrino Detector) anomaly, stemming from an observation of $\overline{\nu}_e$ events in a situation where they should not have been produced originally [15]. The experiment was performed at the Los Alamos Laboratory and involved targeting the primary proton beam on a water target followed by a dense beam dump. The shielding between the target station and the detector ensured that the only significant flux arriving at the detector would be neutrinos. Their dominant source would be π^+ or μ^+ decays. The number of neutrinos from π^- and μ^- decays would be strongly suppressed by the fact that water target strongly favored π^+ production and any π^- produced would be much more likely to stop and be captured rather than decay. Thus, such an experimental situation would give predominantly ν_μ (from π^+ decays) and $\overline{\nu}_\mu$ and ν_e from μ^+ decays. The $\overline{\nu}_e$s would be absent in this scenario.

The experiment looked for possible transformation of $\overline{\nu}_\mu$ into $\overline{\nu}_e$. The signature for $\overline{\nu}_e$ interaction on proton would be detection of the prompt positron from the initial interaction followed by a delayed signal from the neutron capture in liquid scintillator. As is seen in Fig. 13, there was an apparent excess of detected $\overline{\nu}_\mu$s above what one would expect from potential sources such as π^- decays in flight, cosmic rays, accidental coincidences, etc. The background sources could be either directly measured or calculated from other measurements.

The $\overline{\nu}_e$ excess could be interpreted as oscillation of $\overline{\nu}_\mu$s into $\overline{\nu}_e$s. The possible oscillation parameters which can explain this result are illustrated in Fig. 14. All possible values would require Δm^2 which is significantly higher than the two which explain the solar and atmospheric neutrino phenomena. Thus, this would require the fourth neutrino mass state. The only way to reconcile that with the Z° decay result, which showed that there are only three light neutrinos, is to postulate that the fourth neutrino would be sterile, i.e., have no Standard Model interactions.

MiniBooNE experiment was designed to test the LSND result under quite different conditions. An effort was made to cover roughly the same L/E range but the values of both L and E were about an order of magnitude larger. The experiment uses the 8 GeV proton beam from the Fermilab Booster to produce

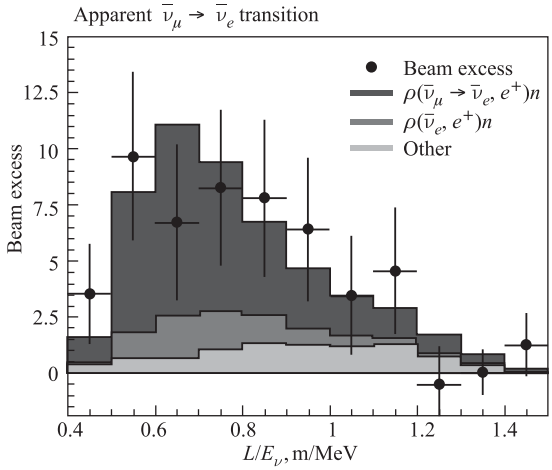

Fig. 13. L/E_ν distribution of the candidate $\overline{\nu}_e$ events in the LSND experiment. The calculated contributions from the different sources are indicated

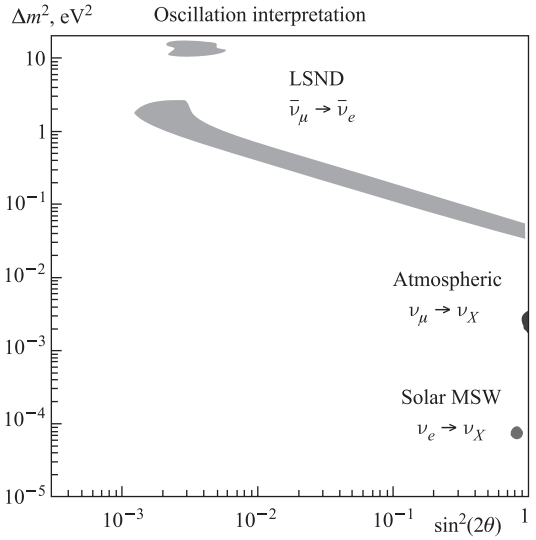

Fig. 14. The region in the oscillation parameters space allowed by the LSND data if the $\overline{\nu}_e$ excess is interpreted as oscillations

the neutrino beam and the detector is similar in its basic nature to the LSND one. It consists of a tank filled with approximately 800 t of mineral oil and lined with photomultipliers recycled from the LSND experiment. The optical signal consists

of Cherenkov light and small amount of scintillator light. The target is inside the magnetic horn whose polarity can be changed to focus either positive or negative secondaries. The drift distance for pion decays is 50 m and is followed by about 500 m of the earth absorber both to stop the muons and to provide potential path length for the oscillations. There is only one (far) detector which is covered with about 3 m of earth overburden to cut out most of the hadronic and electromagnetic component in the cosmic rays and reduce the muon flux by about the factor of 2.

The neutrino beam is mainly ν_μs or $\overline{\nu}_\mu$s depending on the horn polarity. The signal would be ν_es or $\overline{\nu}_e$s, produced by transformation of the muonic component. Thus the experiment faces similar challenges as MINOS in extracting a small ν_e (or $\overline{\nu}_e$) signal in the presence of both NC interactions and beam ν_es. The identification of the signal is also done based on topology even though clearly the variables used here are quite different. Since there is no near detector, one has to rely to a greater extent on Monte Carlo simulations and use of the actual data to generate input necessary for accurate prediction of the background.

The experiment has already taken $6.5 \cdot 10^{20}$ protons on target (POT) with the neutrino beam [16] and is currently running with antineutrinos. To date $5.7 \cdot 10^{20}$ POT have been analyzed from this second data set [17]. The neutrino (antineutrino) energy spectra for events passing all the ν_e ($\overline{\nu}_e$) cuts for the quasieleastic hypothesis are displayed in Fig. 15, *a* and *b*, for neutrinos and antineutrinos, respectively. The contributions to the background from different sources are also indicated showing that the background is dominated by the misidentified π^0s and beam ν_es. In Fig. 15, *a* and *b*, is indicated the region corresponding to the LSND observation of an anomalous signal. There appears to be no excess of events in that region for the neutrino case but there is an excess at energies below the LSND region. The excess could be due to either electrons or gamma rays since the detector cannot distinguish between these two hypotheses. In contrast,

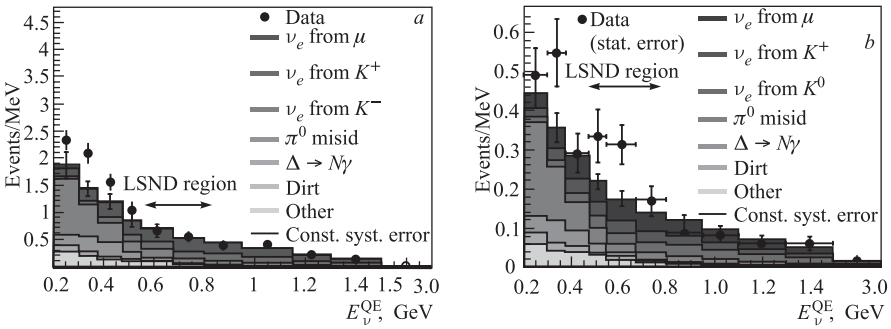

Fig. 15. The observed energy spectra of the candidate ν_e (*a*) and $\overline{\nu}_e$ (*b*) events in the MiniBooNE experiment together with the calculated contributions from the different background sources

the antineutrino data shows an excess of signal events in the LSND region but much smaller excess at low energies, consistent with being due to the neutrino component in the beam. The magnitude of the excess in the antineutrino data in the LSND-relevant energies is consistent with what one would expect from the observed signal in that original experiment.

Various efforts have been made to explain these (and the LSND) data in terms of existence of sterile neutrino(s). Single sterile neutrino appears insufficient to explain all of these data and at least two sterile neutrinos seem to be necessary [18]. The MiniBooNE experiment is in the process of taking more antineutrino data to improve the statistical accuracy of this measurement.

MINOS has performed a search for sterile neutrinos but in a different region of parameter space than investigated by LSND and MiniBooNE. Those experiments are sensitive in the large Δm^2 but small mixing angle domain. On the other hand, MINOS can look in the atmospheric region, i.e., small Δm^2 and relatively large mixing angle [19]. It can thus provide limits on the fraction of ν_μs that might be oscillating into sterile neutrinos. In the conventional picture there should be no depletion of neutral current events since that process does not distinguish between flavors. Thus, MINOS experimental procedure is to look for deficiency of the NC events in the far detector. The specific procedure follows the same path as the CC disappearance analysis. First, NC events are identified in the near detector by the absence of a muon, appearing as a long rack. Subsequently this measurement is used to predict the NC rate in the far detector using the energy-dependent Monte Carlo ratio of far to near detector rates for both the NC signal and the backgrounds.

The spectrum of visible energy for events passing the NC selection cuts, together with the MC prediction, is displayed in Fig. 16. There is a reasonably large uncertainty on the MC prediction, mainly due to the unknowns in the nuclear interaction model. This uncertainty, however, does not affect very much the near/far ratio because of strong correlations in the two detectors and hence the resultant cancellation. The main background, as can be seen from Fig. 16, is the CC background, representing high y events, where the muon is too short to be identified with high level of accuracy. The ν_e CC events would be generally classified as the NC events and thus the interpretation of the results depends on the assumption one makes about the value of θ_{13}.

Figure 17 shows the far detector data together with the prediction based on the near detector measurement. This prediction is shown both for the null value of θ_{13} and for $\theta_{13} = 11.5°$, i.e., the CHOOZ limit. There is no evidence for any depletion of the NC event with respect to the prediction. Quantitatively, we expect to see 757 events (signal + background) assuming no $\nu_\mu \to \nu_e$ conversion and observe 802. We can define

$$R = (N_{\rm data} - N_{\rm bkd})/{\rm signal}_{\rm MC}. \tag{3}$$

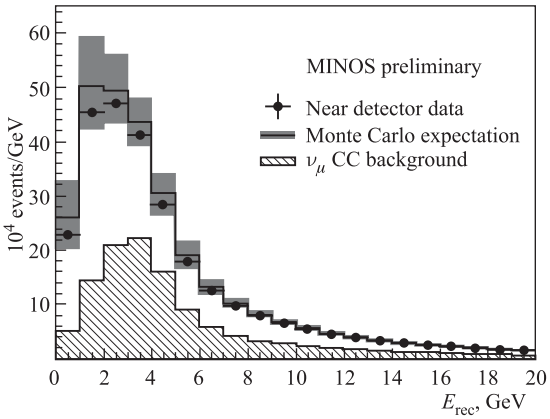

Fig. 16. Energy spectrum of MINOS NC candidate events in the near detector together with the MC calculated expected spectrum and the calculated CC background contribution

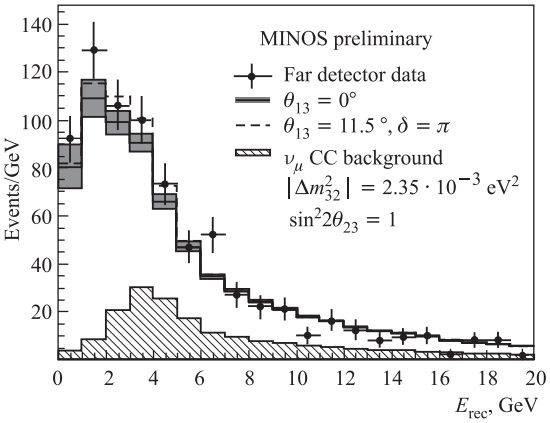

Fig. 17. Energy spectrum of MINOS NC candidate events in the far detector together with the expected spectrum extrapolated from the near detector and with the calculated CC background contribution

Then $R = 1.09 \pm 0.06(\text{stat.}) \pm 0.05(\text{syst.})$. For the fraction of ν_μs which oscillate into sterile neutrinos, defined as

$$f_{st} = \frac{P(\nu_\mu \to \nu_{\rm sterile})}{(1 - P(\nu_\mu \to \nu_\mu))}, \tag{4}$$

we obtain $f_{st} = 0.22(0.40)$ at 90% CL where the number in parentheses corresponds to $\theta_{13} = 11.5°$.

Another potentially very interesting and anomalous result is the measurement of the oscillation parameters by MINOS for $\overline{\nu}_\mu$s [20]. This is the first such measurement in an accelerator produced beam configured to preferentially accept $\overline{\nu}_\mu$s. Both the polarity of the magnetic horns and the direction of the magnetic field in the two detectors have been reversed with respect to the original neutrino configuration. Due to the differences in cross sections and in hadronic production, both of them are favoring neutrinos, the fraction of neutrinos in the antineutrino tuned beam is higher than the reverse situation for a neutrino beam. This is illustrated in Fig. 18. Because of this, more stringent cuts on the muon charge determination have been used in this analysis so as to reduce that potential background in the final event sample. Presence of magnetic field is clearly necessary if one wants to identify antineutrino events on an event-by-event basis.

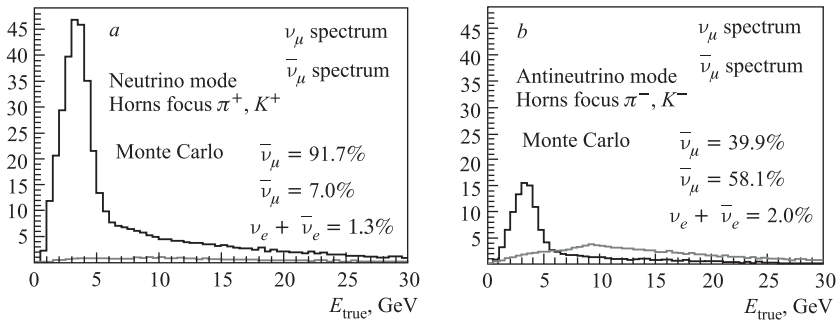

Fig. 18. ν_μ and $\overline{\nu}_\mu$ spectra for the neutrino tuned beam (*a*) and the antineutrino tuned beam (*b*)

The basic analysis procedure is very similar to that used for the neutrino analysis. Near detector data are used to make a prediction as to what one should see in the far detector under different oscillation hypotheses. Likelihood function is then minimized to give the best fit parameters. The muon antineutrino energy spectrum in the far detector for the currently analyzed exposure of $1.7 \cdot 10^{20}$ POT is shown in Fig. 19 together with the prediction from the near detector both on the assumption of no oscillations and for the best fit. The best fit parameters are $\Delta m^2 = 3.36 \cdot 10^{-3}$ eV^2 and $\sin^2(2\theta_{23}) = 0.86 \pm 0.11$. The contours in the 2-dimensional space for both neutrinos and antineutrinos are displayed in Fig. 20. The probability that both sets of data are governed by the same parameters is at a level of 2.3σ.

MINOS is in the process of continuing the antineutrino run with a goal of achieving a total exposure of $4 \cdot 10^{20}$ POT. Clearly, if this result holds up with increased statistics, it would indicate some new physics, either anomalous interaction that is different for neutrinos and antineutrinos [21] or violation of

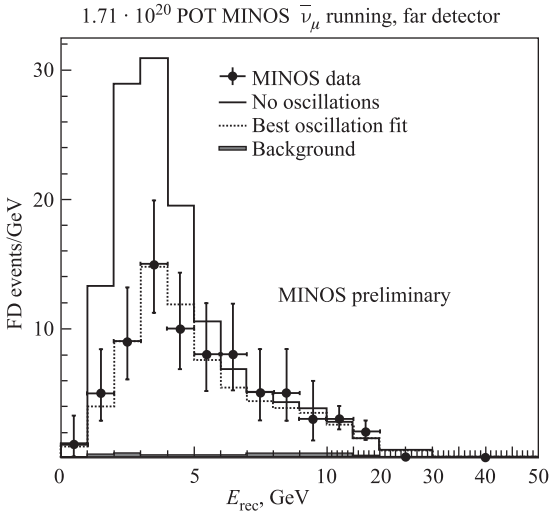

Fig. 19. MINOS CC $\overline{\nu}_\mu$ observed energy spectrum in an antineutrino tuned beam with superimposed no-oscillation and best fit oscillation predictions

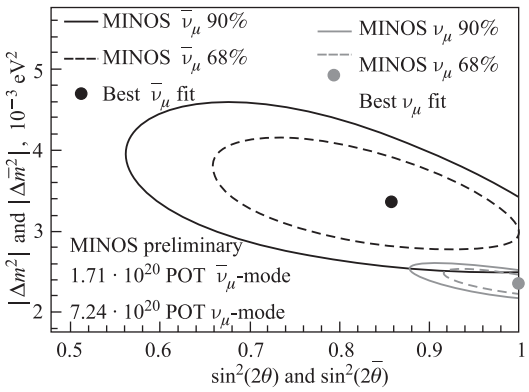

Fig. 20. Allowed contour in the oscillation parameter space for the $\overline{\nu}_\mu$ exposure together with a similar contour for the ν_μ experiment

fundamental symmetries. Parenthetically one should point out that the hypothesis of equal oscillation parameters in the solar sector has not been tested very well. This is because the solar experiments, using neutrinos, constrain the mixing angle very well but the mass squared difference rather poorly. The opposite situation holds true for KamLAND which is observing neutrinos.

5. FUTURE ACCELERATOR EFFORTS (NEAR TERM)

Before discussing future experiments it is useful to summarize the current status of our knowledge of neutrino oscillation in the framework of the standard model of neutrino oscillations. Of the seven parameters describing the oscillations: the three mixing angles, two mass squared differences, CP phase, and the mass hierarchy, four are quite well known today, namely θ_{12} and θ_{23} and the two Δm^2s. Thus the focus of the future experiments is the determination of the other three, initially θ_{13} and then CP phase and mass hierarchy. So far, there is only a limit on θ_{13} (as discussed earlier) but nothing is known about the other two.

There are two near term accelerator efforts designed to address these questions. The first of these is the T2K experiment in Japan [22]. It uses a new neutrino beam based on the extracted protons from the recently constructed JPARC accelerator facility. The beam is aimed at the Super-Kamiokande detector 295 km away. The data taking has already started in 2010 but at a significantly lower intensity than the design value. Significant increase in intensity is anticipated for the forthcoming run.

The other effort is the NOvA experiment based at Fermilab [23]. It will use the NuMI beam line but look at the beam at an off-axis angle. The detector will be brand new and will be located on the surface in Ash River, MN, 810 miles from Fermilab. It is a 14 t, highly segmented liquid scintillator detector with 80% of its mass being active. The detector is currently under construction with the start of data taking with a partial detector scheduled for the latter part of 2012.

The basic goals of both experiments are very similar and focused initially on observation of the $\nu_\mu \to \nu_e$ transition and thus obtaining new information on θ_{13}. Both experiments use off-axis beams optimized for maximum flux near the center of the atmospheric oscillation peak. Because the distances from target location to detectors are quite different in the two cases, the neutrino energy chosen for the T2K experiment is much lower, peaking around 800 MeV, to be compared with the NOvA peak energy around 2.5 GeV. The significantly longer distance used by NOvA gives it some sensitivity to determination of mass hierarchy if θ_{13} is in the range being suggested by some experimental results (as discussed previously).

The layout of the T2K neutrino beam line is shown in Fig. 21. There are three detectors: INGRID is an on-axis detector whose function is to monitor the beam by looking at the muons from neutrino parents. The so-called ND280 detector is an electronic detector, located 280 m from the target, and is designed to study the neutrino interactions in some detail and be able to identify exclusive channels. It will provide detailed input to the Monte Carlo simulations for the far detector, the Super-Kamiokande. Both the ND280 and Super-K are positioned off-axis at 2.5°. The resulting beam at that angle is shown in Fig. 22 which also illustrates the advantage of off-axis configuration when one wants to obtain a reasonably monochromatic beam.

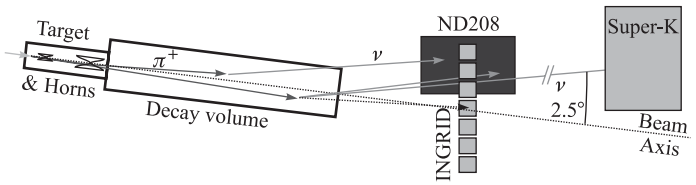

Fig. 21. Schematic of the beam line in the T2K experiment

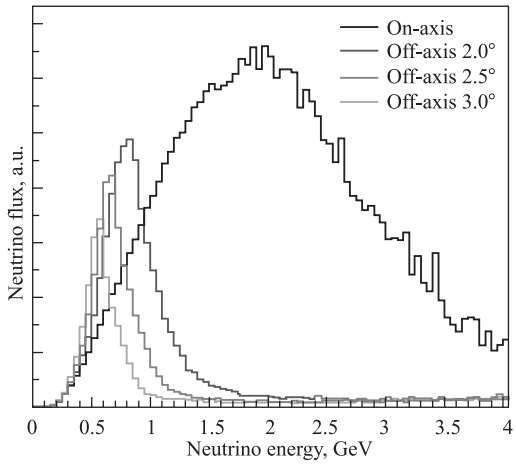

Fig. 22. Neutrino energy spectra from the T2K beam line for the on-axis configuration and various off-axis possibilities

The initial run at the beginning of 2010 was performed at 50 kW, significantly less than the design value of 750 kW. A number of beam upgrades are planned for the next couple of years with a goal of achieving that design value. Probably the most important of these is the increase of the proton linac injector energy. The primary goal of T2K is measurement of θ_{13}. The sensitivity reach of the experiment for a 5 year run at the design intensity is shown in Fig. 23. The sensitivity has a strong dependence on the value of CP parameter δ as can be seen in the Figure but only weak dependence on the mass hierarchy because of the relatively low energy used. The experiment should also be able to improve our knowledge of the oscillation parameters in the atmospheric sector. The advertised values for the full 5 year run are 10^{-4} eV^2 uncertainty on Δm^2 and ability to see deviations from unity of $\sin^2(2\theta_{23})$ up to 0.99.

The NOvA experiment plans to use a novel detector composed entirely of plastic rectangular tubes filled with liquid scintillator. The dimensions of the

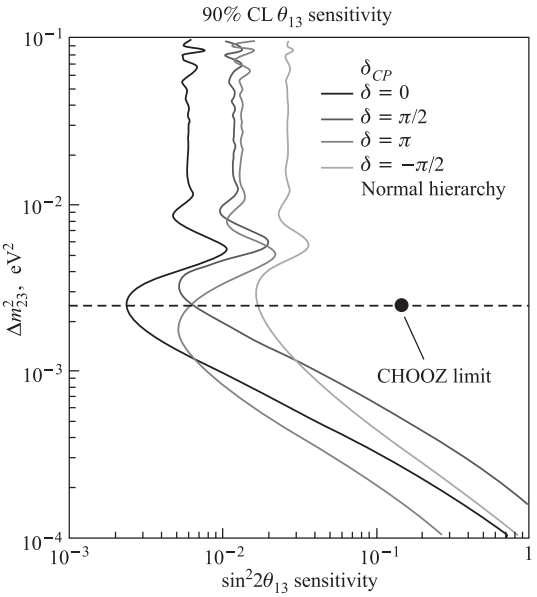

Fig. 23. Sensitivity of the T2K experiment for $\sin^2(2\theta_{13})$ as a function of Δm^2_{23} shown for several values of CP phase δ

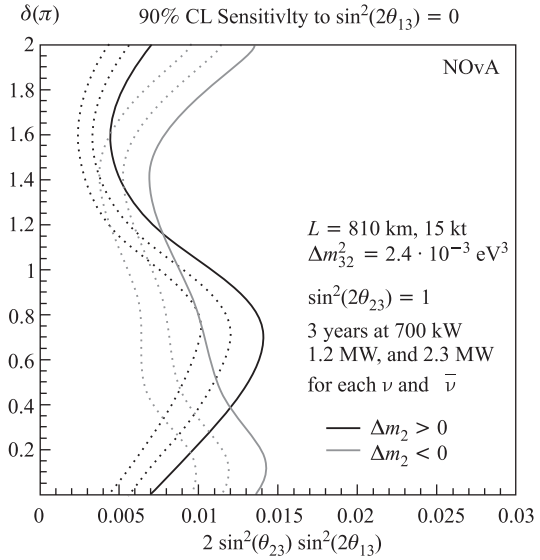

Fig. 24. NOvA sensitivity to $\sin^2\theta_{23}\sin^2(2\theta_{13})$ as a function of CP phase δ for both mass hierarchies and 3 different beam power values. A 3 year run for both neutrinos and antineutrinos is assumed

tubes are 15.7 m long, 4 cm wide and 6 cm deep (along beam direction). That granularity gives longitudinal sampling of $0.2X_0$; a 2 GeV muon will traverse 60 planes. The readout is done by a wavelength shifting fiber that is looped at one end of the cell; at the other end both fiber ends are connected to an APD. The ν_e events will be identified by the presence of an electromagnetic shower

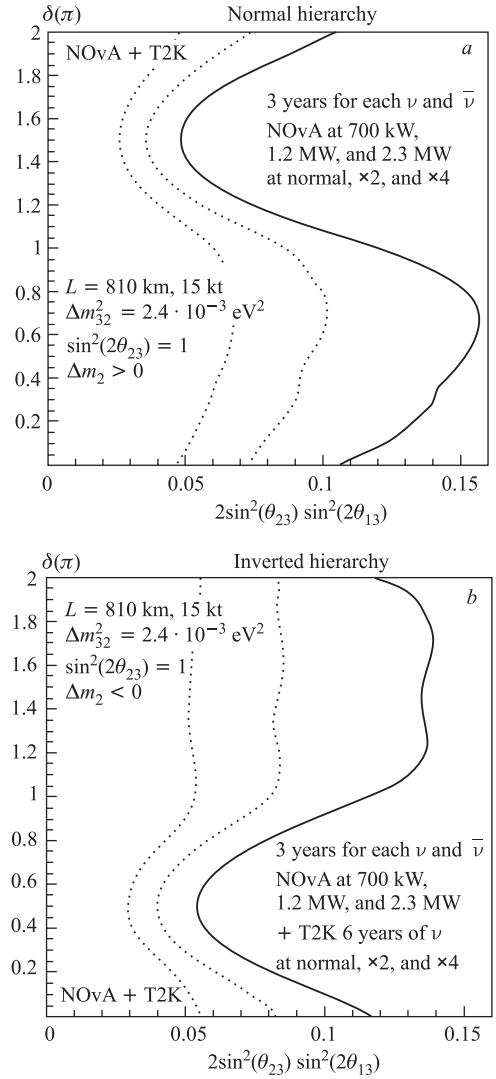

Fig. 25. Sensitivity of the combined data from the NOvA and T2K experiments for the determination of the mass hierarchy

along the electron track, i.e., relatively narrow band of energy deposition but one that extends over several neighboring cells. The total tonnage of the detector is 14 kt; its total length 67 m.

There will also be a near detector which is essentially a smaller replica of the main detector except that it will have iron plates at the back to range out all the muons in the interesting energy range. It will be located in the NuMI tunnel, about 1 km from the target. A prototype of its active part has been assembled on the surface and is currently taking data from the NuMI beam running antineutrinos. Its current location corresponds to a 110 mr off-axis angle with respect to the NuMI beam line.

The far detector is on a green site in Ash River, MN, so the experiment required significant site preparation before its construction could begin. The most important part of that phase is now complete and assembly of the detector should begin before the end of 2011. The detector is 810 km from the target, 14 mrad off-axis from the NuMI beam line. The NuMI beam line will be tuned to medium energy and the resulting spectrum in this configuration will be peaked around 2.5 GeV. As in the T2K experiment, the high energy neutrino flux will be strongly suppressed improving significantly signal to background ratio. The current plans for NOvA contemplate a 3 year run on neutrinos and a 3 year run on antineutrinos with beam power of 700 kW. The sensitivity to the mixing angle is displayed in Fig. 24. The ability to distinguish between the two mass hierarchies can be enhanced by doing a joint analysis of both the NOvA and T2K data sets. The fact that T2K is relatively insensitive to the mass hierarchy allows such an analysis to resolve some of the intrinsic ambiguities. The reach for mass hierarchy determination is shown in Fig. 25.

6. FUTURE PLANS (LONG TERM)

The current plans for programs beyond T2K and NOvA are still not very well defined. On a shorter time scale they involve significant upgrades to accelerators, neutrino beam lines, and detectors with a goal to significantly increase neutrino event rates. On a longer time scale there is an active research and development program around the world to develop new accelerator facilities like neutrino factories and beta beams. Discussion of these plans is beyond the scope of this report but a short review of the more immediate plans seems appropriate.

At this time, the future US program appears to be somewhat better defined than those in Asia and Europe. It is centered around eventual development of two new major facilities: a new underground laboratory and a new accelerator complex at Fermilab. The underground laboratory is the Deep Underground Science and Engineering Laboratory (DUSEL) to be developed at the former Homestake mine in Lead, South Dakota. The new accelerator facility is referred

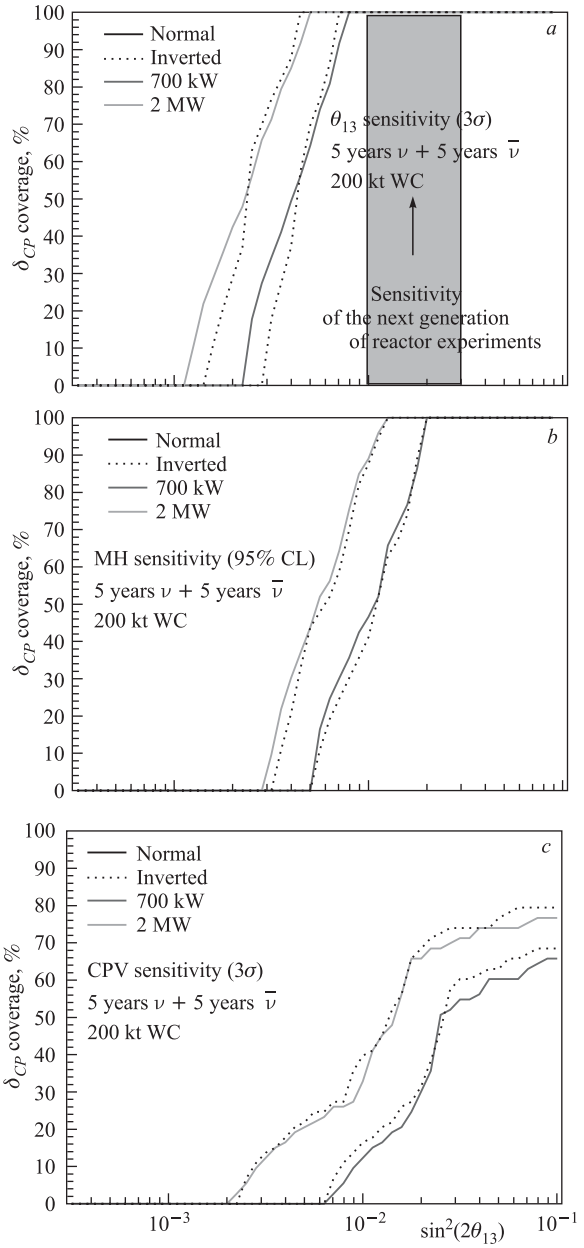

Fig. 26. Sensitivity of the LBNE experiment for detection of nonzero $\sin^2(2\theta_{13})$, for determination of the mass hierarchy and for observation of CP violation

to as Project X. It is a major upgrade of the Fermilab Main Injector achieved by replacement of the current 8 GeV Booster by an 8 GeV superconducting linac. Neither project is funded as of this date but the hope is that DUSEL project can be completed before the end of this decade and the Project X a few years later.

The first phase of this program would be the Long Baseline Neutrino Experiment (LBNE). It would require a new neutrino beam line aimed at DUSEL, about 1365 km away. Initially the beam would be operated at 700 kW but would be designed with a possibility of upgrade to an eventual power of 2 MW, expected to become feasible with the Project X.

The initial detector would be either a 100 kt fiducial mass water Cherenkov detector or an equivalent (about 17 kt) liquid argon detector. The laboratory would be designed so that additional detectors could be added later. The potential sensitivities for $\sin^2(\theta_{13})$, determination of mass hierarchy, and significant observation of CP violation are shown for two different beam intensities in Fig. 26.

The long range program in Asia is centered around an upgrade of the JPARC accelerator to 2.5 MW. Furthermore, the current beamline would be used in association with a new detector (or detectors) in the 0.5–1 Mt range. Several location/detector options are being considered ranging from a single large water Cherenkov detector near the current Super-K site to a large liquid argon detector on the island of Okinoshima, 658 km from the neutrino source, or two detectors separated by about 1000 km, one at the current Super-K site and the other one in Korea. Even though both water and liquid argon detectors are being considered, the water Cherenkov detector seems to be the preferred option today.

European long range plans in neutrino physics are even more uncertain mainly due to the fact that over the past few years the main focus there has been the LHC issues. There has been an ongoing study as to the best course to pursue and this work is supposed to be completed in 2011. In parallel there is going on an evaluation of seven potential sites for an underground laboratory.

7. CROSS SECTIONS

In the past, the major focus of neutrino cross section experiments has been studies of structure functions and measuring the fundamental parameters of the Standard Model. Today, the emphasis has shifted more towards investigations of intranuclear processes and providing important input for the oscillation experiments besides studying some fundamental processes like quasielastic scattering and coherent pion production. As discussed earlier, measurement of neutrino cross sections is difficult because of problematic issues associated with the determination of neutrino flux. Furthermore, the relative coarseness of most neutrino detectors makes studies of exclusive reactions and their properties difficult.

In principle, at least determination of the neutrino flux can be made in one of three ways. Production of hadrons can be measured in auxiliary experiments and the neutrino flux deduced from those results and from the beam geometry and focusing arrangements. Alternatively, flux can be determined by measuring the rate for a process whose cross section is known reliably from theory [24]. Finally, one can measure the flux of the decay muons. All of these methods have been tried in the past but none of them is easy. The existing problems with flux normalization are shown in the two graphics in Fig. 27, the plot *a* showing the measured quasielastic cross sections by different experiments, the plot *b* the

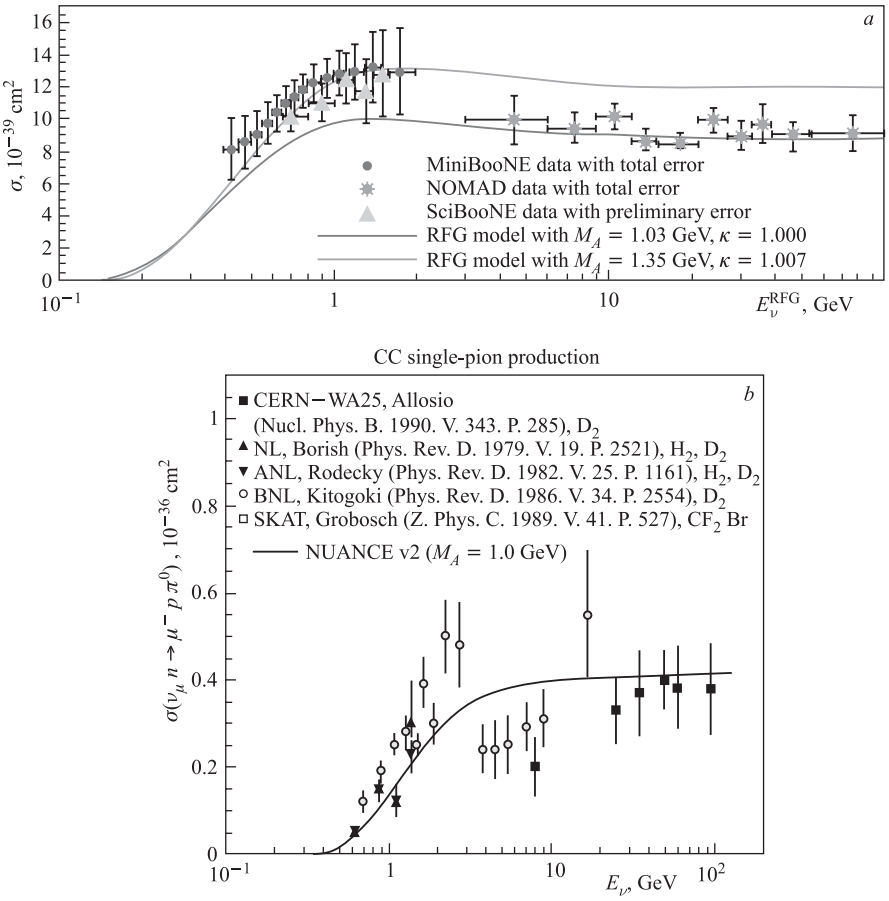

Fig. 27. Currently available data on the quasielastic ν_μ cross section (*a*) and on inclusive π^0 production (*b*)

inclusive pion production in the CC interactions. The lack of continuity in the data points to some uncertainty in the normalization of different experiments.

Today some progress is being made in the cross section studies by virtue of high statistics data samples in the near detectors of MINOS [24] and K2K [25], experiments with close by detectors like MiniBooNE [26] and dedicated cross section experiments like SciBooNE [27] and MINERvA [28]. Space does not allow me to discuss properly the results from these experiments. The current overall situation for total CC cross sections is shown in Fig. 28, where the older data points are augmented by the recent MINOS measurement.

Detailed understanding of some processes can be helped by the knowledge of exclusive reactions. Thus, for example, determination of $\nu_\mu \to \nu_e$ rate relies at some level on accurate determination of the background. More specifically,

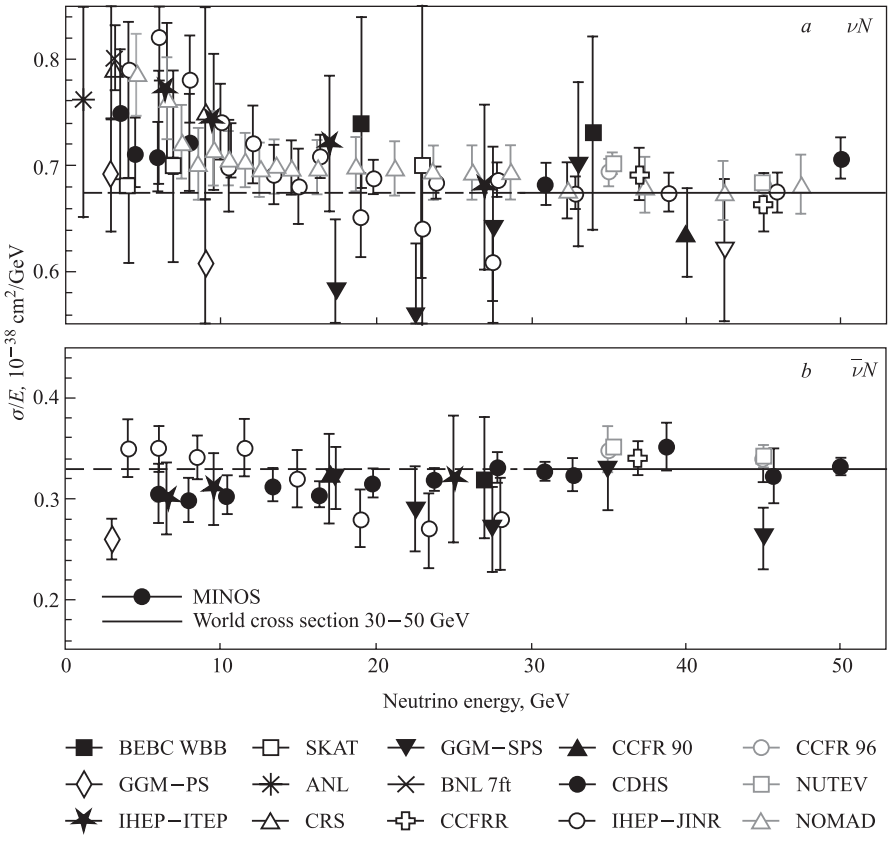

Fig. 28. Currently available data on the total CC ν_μ (*a*) and $\overline{\nu}_\mu$ (*b*) inclusive cross sections

it helps to know the rate and details for such reactions as resonance production and inclusive π^0 production, the chief source of background for this transition mode. The current knowledge, which forms an important input to the simulation programs, is rather poor. This is illustrated in Fig. 29 where we show the prediction from the NUANCE code regarding the invariant cross sections for the isobar production as a function of its mass and for the inclusive charged current π^0 production as a function of its momentum together with the results from the MiniBooNE experiment [29].

In the near future, we can look forward to rather detailed data in the medium energy range from the MINERvA experiment and from the ND280 near detector in T2K. Both of these are very fine grained detectors that will be exposed to very

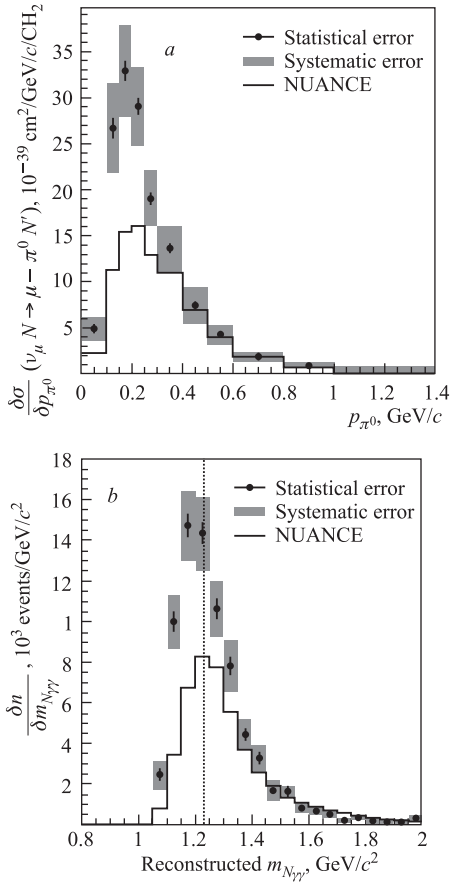

Fig. 29. Comparison of the NUANCE predictions with the MiniBooNE data for π^0 production (*a*) and production of nucleon-π system (*b*)

intense neutrino flux. Thus they should be able to provide detailed information on many exclusive channels of interest. ND280 would be sensitive mainly to the neutrino energies in the sub-GeV range whereas MINERvA would explore mainly the few GeV region.

8. SUMMARY

Over the last 12 years, since the discovery of neutrino oscillations in 1998, a great progress has been made in understanding that phenomenon. But a number of key questions are still awaiting answers. The accelerator based neutrino experiments have provided important and extensive information in these studies in the past. There is no doubt that they will continue to do so in the future. The technical advances in detectors, neutrino beams and in accelerators have played important role in advancing the capabilities of these experiments and will certainly continue to do so.

REFERENCES

1. *Pontecorvo B.* // JETP. 1959. V. 37. P. 1751.
2. *Schwartz M.* // Phys. Rev. Lett. 1960. V. 4. P. 306.
3. *Danby G. et al.* // Phys. Rev. Lett. 1962. V. 9. P. 36.
4. *Ahn M. H. et al. (K2K Collab.)* // Phys. Rev. D. 2006. V. 74. P. 072002.
5. *Adamson P. et al. (MINOS Collab.)* // Phys. Rev. D. 2008. V. 77. P. 072002.
6. *Michael D. et al. (MINOS Collab.)* // Nucl. Instr. Meth. A. 2008. V. 596. P. 190.
7. *Adamson P. et al. (MINOS Collab.)* // Phys. Rev. Lett. 2010. V. 283. P. 367.
8. *Ashie Y. et al. (SuperKamiokande Collab.)* // Phys. Rev. Lett. 2004. V. 93. P. 10181.
9. *Ashie Y. et al. (SuperKamiokande Collab.)* // Phys. Rev. Lett. 2005. V. 71. P. 112005.
10. *OPERA Collab.* // Nucl. Phys. Proc. Suppl. 2007. V. 168. P. 173;
Guler M. et al. (OPERA Collab.). CERN SPSC. 2001-025.
11. *Agafonova N. et al. (OPERA Collab.)* // Phys. Lett. B. 2010. V. 691. P. 138.
12. *Apollonio M. et al. (CHOOZ Collab.)* // Eur. Phys. J. C. 2003. V. 27. P. 331.
13. *Fogli G. L. et al.* // Phys. Rev. Lett. 2008. V. 101. P. 141801;
Schwetz T., Tortola M., Valle J. W. F. // New J. Phys. 2008. V. 10. P. 113011.
14. *Adamson P. et al. (MINOS Collab.)* // Phys. Rev. Rapid Commun. D. 2010. V. 82. P. 051102.
15. *Aguilar A. et al. (LSND Collab.)* // Phys. Rev. D. 2001. V. 64. P. 112007.
16. *Aguilar-Arevalo A. A. et al. (MiniBooNE Collab.)* // Phys. Rev. Lett. 2009. V. 102. P. 101802.

17. *Aguilar-Arevalo A. A. et al. (MiniBooNE Collab.)* // Phys. Rev. Lett. 2010. V. 105. P. 181801.

18. *Karagiorgi G. et al.* // Phys. Rev. D. 2010. V. 80. P. 073001.

19. *Adamson P. et al. (MINOS Collab.)* // Ibid. V. 81. P. 052004.

20. *Vahle P. (for MINOS Collab.)*. Invited paper presented at the 2010 Neutrino Conference, Athens, Greece.

21. *Wolfenstein D. L.* // Phys. Rev. D. 1978. V. 17. P. 2369;
Valle J. W. F. // Phys. Lett. B. 1987. V. 199. P. 432;
Gonzalez-Garcia M. C. et al. // Phys. Rev. Lett. 1999. V. 82. P. 3202;
Friedland A., Lundardini C., Maltoni M. // Phys. Rev. D. 2004. V. 70. P. 111301.

22. *Ytow Y. et al. (T2K Collab.)*. hep-ex/0106019v1. 2001.

23. *Ayers D. et al. (NOvA Collab.).* hep-ex/0403053v1. 2005.

24. *Adamson P. et al. (MINOS Collab.)* // Phys. Rev. D. 2010. V. 81. P. 072002.

25. *Ahn M. H. et al. (K2K Collab.)* // Phys. Rev. D. 2006. V. 74. P. 072003;
Nakayama Y. et al. (K2K Collab.) // Phys. Lett. B. 2005. V. 619. P. 255;
Gran R. et al. (K2K Collab.) // Phys. Rev. D. 2006. V. 74. P. 052002.

26. *Aguilar-Arevalo A. A. et al. (MiniBooNE Collab.)* // Phys. Rev. Lett. 2007. V. 100. P. 032031.

27. *Kurimoto Y. et al. (SciBooNE Collab.)* // Phys. Rev. D. 2010. V. 81. P. 033004.

28. *Drakoulakos D et al. (MINERvA Collab.)*. hep-ex/0405002.

29. *Aguilar-Arevalo A. A. et al. (MiniBooNE Collab.)* // Phys. Rev. D (submitted); hep-ex/1010.3264. 2010.